0022–3530/94 $3.00

Magnesian Andesites and the Subduction Component in a Strongly Calc-Alkaline Series at Piip Volcano, Far Western Aleutians

by G. M. YOGODZINSKI[1], O. N. VOLYNETS[2], A. V. KOLOSKOV[2], N. I. SELIVERSTOV[3], AND V. V. MATVENKOV[4]

[1]*Department of Geological Sciences & INSTOC, Cornell University, Ithaca, New York 14850*

[2]*The Institute of Volcanic Geology and Geochemistry, Petropavlovsk, Kamchatka 683006, Russia*

[3]*The Institute of Volcanology, Petropavlovsk, Kamchatka, 683006, Russia*

[4]*The Institute of Oceanology, Moscow, 117218, Russia*

(*Received 6 July 1992; revised typescript accepted 6 April 1993*)

ABSTRACT

Piip Volcano is a hydrothermally active seamount located in the strike-slip regime immediately north of the far Western Aleutian Ridge. Fractionation of hydrous and oxidized magnesian andesites (MA) produced an igneous rock series at Piip Volcano with a lower average FeO*/MgO (more strongly calc-alkaline) than any in the Central or Eastern Aleutian arc. Basaltic rocks in the Piip Volcano area are rare, and those that do occur have characteristics transitional toward MA (high SiO_2 and Na_2O; low CaO/Al_2O_3). The compositions of the MA and their predominance as parental magmas throughout the Western Aleutians since Middle Miocene time suggest that transpressional tectonics causes primitive basaltic melts of the mantle wedge to pool immediately below the arc crust, where they interact with warm, ambient peridotite to produce highly silica-oversaturated lavas of mantle origin. Proposed consequences of a long melting column in the mantle wedge (e.g., high percentage melting and tholeiitic volcanism) are not observed at Piip Volcano, despite that fact that it is built on very thin crust.

Arc-related incompatible element signatures in volcanic rocks of the Piip Volcano area (e.g., high Ba/La, La/Sm, and Th/Ta) are broadly transitional between mid-ocean ridge basalt (MORB) and basalts of the Central and Eastern Aleutians. Interelement and isotopic ratios are, however, MORB-like ($^{206}Pb/^{204}Pb < 18{\cdot}2$, $\varepsilon_{Nd} > 10$, $^{87}Sr/^{86}Sr < 0{\cdot}7028$). Mixtures of hypothetical slab melts (Western Aleutian adakite) and depleted MORB mantle produce an enriched peridotite source with incompatible element and isotopic characteristics of the Western Aleutian rocks. Components from recycled marine sediment (e.g., radiogenic Pb) are absent, possibly because they have been stripped out at shallow levels by the long, oblique subduction path beneath the forearc. The incompatible element signatures of the Western Aleutian rocks (including Ta depletion) are largely inherited from small percentage melts of the subducting slab, which enrich the mantle wedge source. Fluid-dominated processes of mass transport are not required to explain the arc-type incompatible element signature of the Western Aleutian rocks.

INTRODUCTION

Magmatic activity caused by lithospheric plate subduction is the key to our understanding of arc tectonics, the formation of the continental crust, and the characteristics of the modern

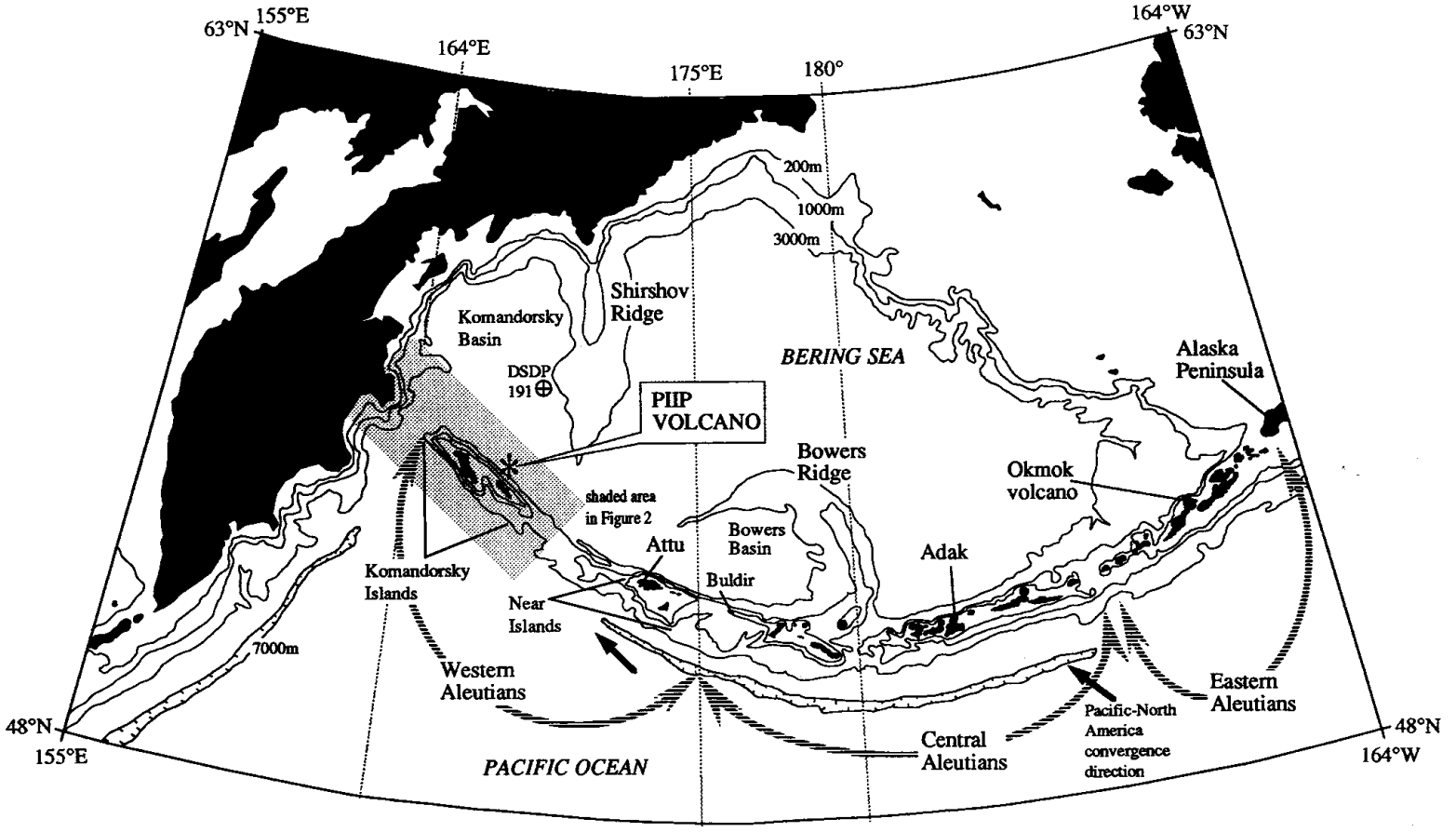

FIG. 1. Insular Aleutian arc and surrounding region. Modern Pacific–North America convergence in the Western and Central Aleutians (N49W, 92 mm/yr, and N42W, 87 mm/yr, respectively; Engebretson *et al.*, 1985). Piip Volcano, located in the far western arc, is a hydrothermally active seamount (Seliverstov *et al.*, 1990; Baranov *et al.*, 1991). Shaded area is detailed in Fig. 2.

crust–mantle geochemical system. Among the important aspects of subduction zone magmatism that continue to be of interest are: (1) the nature of primitive arc magmas, (2) the origin of the calc-alkaline series, and (3) the origin of the subduction geochemical signature (e.g., Tatsumi *et al.*, 1986; Kelemen, 1990; Kelemen *et al.*, 1990; Morris *et al.*, 1990; Stern *et al.*, 1991; Miller *et al.*, 1992; Kay & Kay, in press).

In the Aleutians (Fig. 1), the study of these and related topics has been directed primarily at the Central and Eastern arc (defined here as 164°W–175°E longitude), where there is a well-developed magmatic front and Wadati–Benioff Zone. In contrast, the Western Aleutian arc (defined here as 164°E–175°E longitude) is dominated by strike-slip tectonics, and is both volcanically less active and less well studied. The youngest magmatic rocks in the Western Aleutian Near and Komandorsky Islands (Fig. 1) are Late Miocene to Pliocene in age (DeLong & McDowell, 1975; Borusk & Tsvetkov, 1982; Tsvetkov, 1991; Vallier *et al.*, in press), but dredging and seafloor imaging have shown that there is an active front of seafloor magmatism along the northern margin of much of the Western Aleutian bathymetric ridge (Scholl *et al.*, 1976; Seliverstov *et al.*, 1990; Baranov *et al.*, 1991).

The clearest case of active magmatism in the Western Aleutians is that of Piip Volcano—a small, hydrothermally active seamount located within the strike-slip regime immediately north of the far Western Aleutian Komandorsky Islands (Figs. 1 and 2; see also Seliverstov *et al.*, 1990; Baranov *et al.*, 1991; Tsvetkov, 1991; Romick *et al.*, in press). Here, we present the results of a petrological and geochemical study of Late Pliocene(?) and Pleistocene-to-Recent volcanic rocks from the Piip Volcano area. We emphasize the origin of magnesian andesites in the Western Aleutians with implications for the calc-alkaline igneous rock series, and the importance of slab melting in the Western Aleutians with implications for the subduction geochemical signature in arc magmas.

REGIONAL TECTONICS AND GEOLOGIC FRAMEWORK OF THE WESTERNMOST ALEUTIAN RIDGE

In the modern Aleutian arc, the Pacific–North America convergence angle, and the rate of convergence, decreases from east to west (Fig. 1). The general seismic, structural, and magmatic character of the Western Aleutian region has led some workers to conclude that a subducting slab is not present beneath the Western Aleutian ridge (e.g., Newberry *et al.*, 1986). This conclusion has substantially influenced geochemical interpretations of Western Aleutian volcanic rocks (Romick *et al.*, in press). It has become increasingly clear, however, that in many arcs a relatively cold subducting slab penetrates to depths well beyond the active seismic zone. Boyd & Creager (1991) have imaged the aseismic extension of the Aleutian slab to depths of at least 600 km along all segments of the insular arc. Despite the nearly pure transform motion between the Pacific and North American plates along the Western Aleutian plate boundary, oblique subduction in the Central Aleutians over the past 15–20 Ma has apparently carried a subducting slab to great depths beneath the Western Aleutian–Bering Sea region (Creager & Boyd, 1991).

The structure of the westernmost Aleutian ridge and adjacent Komandorsky Basin is dominated by two large right-lateral faults, the Bering and Alpha faults (Fig. 2), which have formed in response to arc-parallel Pacific–North America plate motion (Seliverstov *et al.*, 1990; Baranov *et al.*, 1991). The Bering Fault is expressed by the steep northern slope of the Western Aleutian ridge and by a deep bathymetric depression that extends northwest to the Kamachatka Peninsula. The Alpha Fault parallels the Bering Fault, ~60–80 km to its northeast, from the southern end of the Shirshov Ridge to the Kamchatka Peninsula (Figs. 1

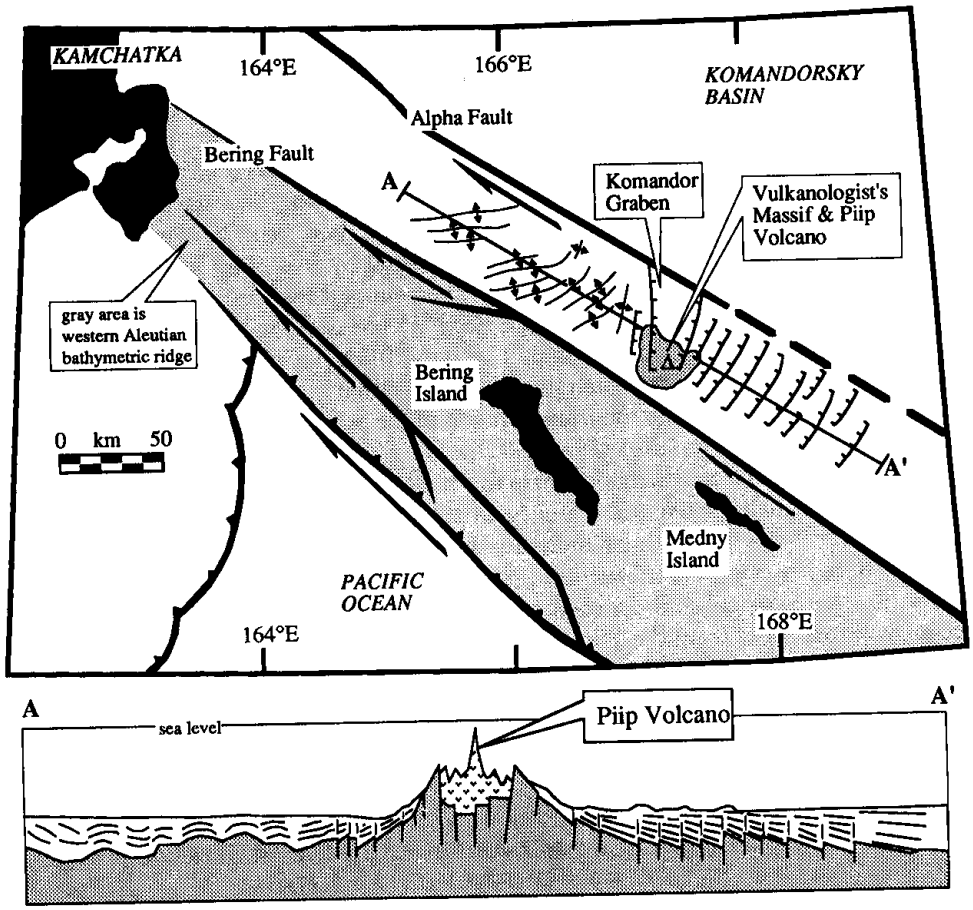

FIG. 2. Tectonic interpretation of the Aleutian–Kamchatka junction modified from Volynets *et al.* (1992). Bathymetric and seismic data for this region are from Baranov *et al.* (1991). Location of the Vulkanologist's Massif is marked approximately by the 3500-m bathymetric contour (see Fig. 3). Piip Volcano (shown by small triangle) is located within the southern Komandor Graben. Hash-marked lines immediately southeast of the Komandor Graben represent normal faults; symbols to northwest of the Komandor Graben are fold axes. These are interpreted in the cross-section (A–A').

and 2). The level of seismicity on these structures and their youthful bathymetric expression indicates that they are among the most active in the region.

The Bering and Alpha faults bound a crustal block in the southermost Komandorsky Basin that has a geophysical expression distinct from crust of the main Komandorsky Basin to the north and the Aleutian bathymetric ridge to the south (Seliverstov *et al.*, 1990; Baranov *et al.*, 1991). North of Medny Island (Fig. 2), this crustal block is cut by a series of NS–NNE-trending normal faults, the largest of which bound a structural depression termed the Komandor Graben. These dilational structures are thought to be late Quaternary in age because they penetrate the uppermost sedimentary cover and because their bathymetric expression is well developed despite intense terrigenous sedimentation. Northwest of the Komandor Graben, the layered sedimentary section is deformed into a series of ENE–NE-trending drape folds over acoustic basement highs. The structural shortening implied by these folds apparently has resulted from spreading across the Komandor Graben and to its SE (Fig. 2).

Recent volcanism in this area is concentrated within a broad bathymetric high termed the Vulkanologist's Massif (Seliverstov *et al.*, 1990; Baranov *et al.*, 1991), which encompasses the southern end of the Komandor Graben (Figs. 2 and 3). This bathymetric high was originally

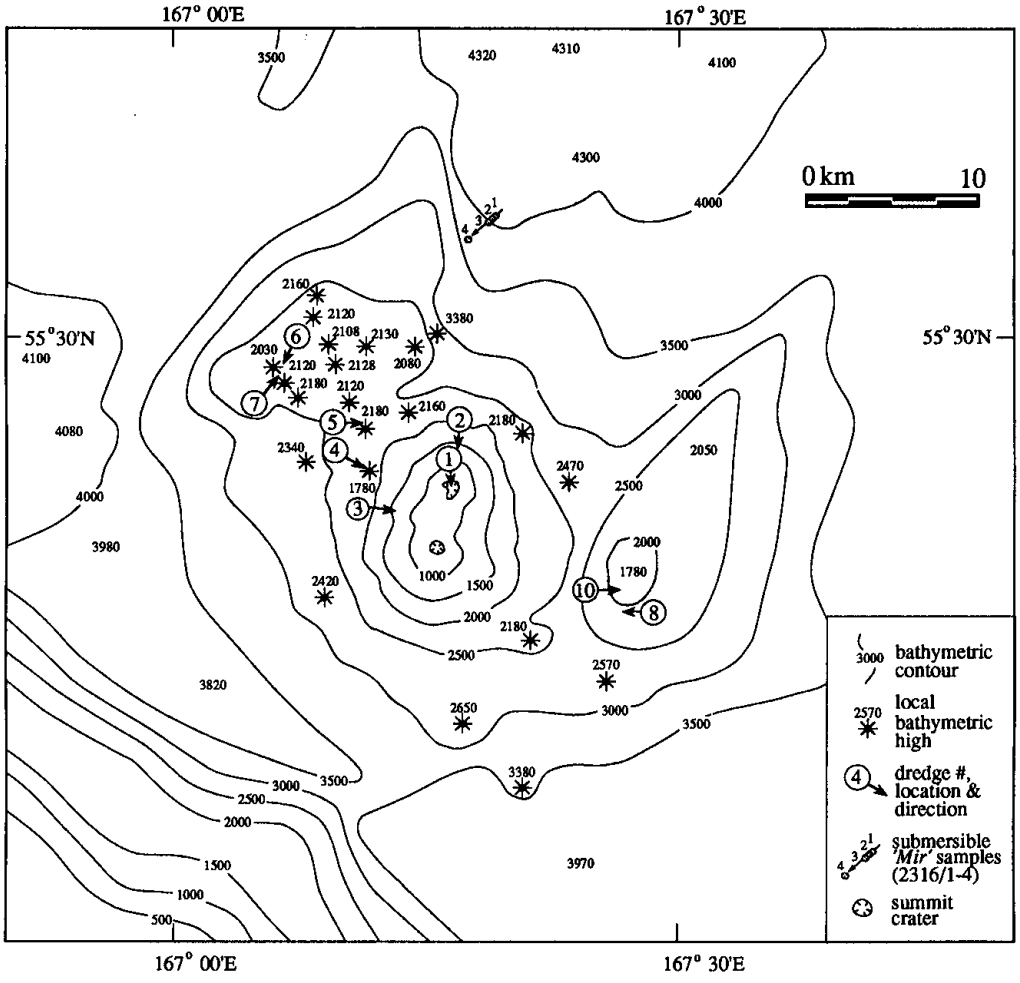

FIG. 3. Bathymetry of the study area, showing dredge locations and locations of samples collected by the submersible *Mir*. Modified from Volynets *et al.* (1992).

thought to be a constructional edifice of young volcanic rock, but dredging has now recovered a series of older (Plio-Pleistocene?) volcanic rocks from the margins of the Komandor Graben. At the southern end of the Komandor Graben, Piip Volcano rises from ~2000 m depth to within 600 m of the sea surface (Fig. 3). According to the estimate of Boyd & Creager (1991), Piip Volcano is located 100–130 km above the subducting slab. The summit of the volcano is composed of three coalescing cones which are aligned north–south. The northern and southern cones have craters of 300–500 m in diameter open to the southwest, and the northern cone is hydrothermally active with 'black smoker' chimneys several meters in height.

Piip Volcano is located on crust of the southernmost Komandorsky Basin where the back-

arc crust adjoins that of the arc (Fig. 2; see also Seliverstov *et al.*, 1990; Baranov *et al.*, 1991). This position is not substantially different from that of Central Aleutian volcanoes which reside at the northern limit of the Central Aleutian ridge crest. Only in the Eastern Aleutians and on the Alaska Peninsula does the magmatic front coincide (approximately) with the bathymetric crest of the Aleutian Ridge. Thus in the Western Aleutians there is a structural arc (the Aleutian bathymetric ridge) and there is a Western Aleutian magmatic front that is displaced slightly to its north (see also Seliverstov *et al.*, 1990; Baranov *et al.*, 1991).

SERIES DEFINITION AND SAMPLE/DREDGE LOCATION

Data presented here are principally from dredge samples taken by the Soviet research vessel *Vulkanolog* on Leg 35 of its 1989 cruise (sample series 35 in Table 1). These samples are grouped into the Piip Series and Komandor Series, on the basis of sample location and apparent relative age. Dredge locations are shown in Fig. 3. Dredge descriptions are given in the Appendix.

Rocks of the Piip Series were dredged from Piip Volcano proper (dredges 1–3, 600–1500-m depth) and from small extrusions at the volcano's base (dredges 4 and 5, ~2100-m depth). The Piip Series is assumed to be < 700 000 years old, on the basis of the magnetic signature of the volcano, but the fresh surface of the northern cone (free of ice-rafted debris), suggests that this part of the volcano has been constructed in Holocene time (Seliverstov *et al.*, 1990; Baranov *et al.*, 1991). Rocks of the Komandor Series were dredged from the Vulkanologist's Massif along margins of the Komandor Graben at depths of 1800–2200 m (dredges 6–8 and 10, Figs. 2 and 3). Many of these were coated by manganese rinds (up to 1·5 cm thick), and are assumed largely to predate the main edifice of Piip Volcano.

In addition to the Leg 35 dredge samples, analyses of four rocks collected in 1990 by the Soviet submersible *Mir* on Leg 23 of the cruise of the research vessel *Akademik Keldish* are also included (sample series 2316, Table 1). These samples were collected at depths of 4200–3500 m from pillow lavas along the western margin of the Komandor Graben (Fig. 3). They are petrographically fresh, but their ages relative to dredge samples are not known. They have been grouped with the Komandor or Piip Series on the basis of compositional similarities only.

MAJOR ELEMENTS—MINERALOGY

Most of the Western Aleutian samples are petrographically fresh. Piip Series rocks contain only occasional veinlets of palagonitic alteration. Some Komandor Series rocks are more altered, but this is generally limited to hydration and devitrification of groundmass glass. Low-grade metamorphic minerals (chlorite, sericite, zeolites, etc.) appear to be absent. Petrographic and primary mineralogic data are summarized in Tables 2 and 3. Mineral analyses have been published elsewhere (Volynets *et al.*, 1992; Romick *et al.*, in press).

The Komandor Series (basalts, basaltic andesites, and andesites)

The Western Aleutian Komandor Series is a medium-K calc-alkaline series (low FeO*/MgO relative to SiO_2; Fig. 4) that is composed mostly of andesite (56–58% SiO_2), but includes minor amounts of basalt ($SiO_2 < 52\%$), and basaltic andesite (52–55% SiO_2; Fig. 4). Komandor Series rocks have relatively low FeO*/MgO (1·1–1·5), with MgO contents of 5–6% in the basalts, 4·5–5·0% in the basaltic andesites, and 3·5–4·5% in the andesites (Fig. 5). The basalts and andesites have low TiO_2 (0·6–1%), but the basaltic andesites range to

higher values (up to 1·5% TiO_2; Fig. 5). All of the Komandor Series rocks have relatively high Al_2O_3 (17–19%) and Na_2O (3·4–4·1%), and in this respect they are similar to the younger Piip Series (see below). Komandor Series rocks are, however, distinct from most high-Al basaltic rocks of the Central and Eastern Aleutians where FeO*/MgO > 1·5 is common (e.g. Table 2 of Kay & Kay, in press).

The predominance of Mg-rich mafic phenocrysts in the Komandor Series rocks is consistent with the low whole-rock FeO*/MgO, and high anorthite content in plagioclase phenocrysts, suggesting broad equilibrium beween whole-rock and phenocryst compositions (Table 2, and Volynets *et al.*, 1992). Basalts, basaltic andesites, and andesites all have phenocrysts of olivine, clinopyroxene, and plagioclase. Available data indicate that the mafic phenocrysts are Mg rich (up to *mg*-number 89), plagioclase phenocrysts are calcic (up to An_{83}; Table 2), and normal compositional zonation predominates. Chromian spinel inclusions, which occur within olivine phenocrysts of the basalts only, have relatively aluminous compositions, similar to those in abyssal peridotites (Fig. 6).

The Piip Series (magnesian andesite to rhyodacite)

Magnesian andesites (MA) are the least evolved rocks in the Piip Series, and have among the lowest FeO*/MgO (0·7–0·9) of any Aleutian volcanic rocks (e.g., Table 1 of Kay & Kay, in press). The Piip Series MA have moderate MgO contents (~6%), low CaO (7–8%), and high Na_2O (3·6–4·1%) and Al_2O_3 (16·5–17·7%). The remainder of the Piip Series show increasing K_2O and Na_2O, and decreasing FeO*, MgO, CaO, Al_2O_3, TiO_2, and CaO/Al_2O_3 with increasing SiO_2 (Figs. 4 and 5). High Fe_2O_3/FeO in Piip Series lavas of all compositions indicate a relatively oxidized mantle source (0–2 log units above NNO; see Luhr & Carmichael, 1985; Lange & Carmichael, 1990; Carmichael, 1991). Anomalously high H_2O^+ contents (> 1%) in some samples may reflect minor hydrous alteration, but the presence of amphibole in all samples with > 59% SiO_2 indicates a high water content in Piip Series magmas.

Mafic phenocryst compositions in the MA confirm that they are near-primary melts of the sub-arc mantle. The Piip Series MA are crystal poor, with 1–6 modal % phenocrysts of olivine ($Fo_{87-91·5}$) and clinopyroxene (*mg*-number 84–90) in an intersertal groundmass of glass, orthopyroxene (up to En_{86}), olivine, and plagioclase (Fig. 7, and Tables 2 and 3). The Mg-rich mafic phenocrysts are approximately at equilibrium with whole-rock compositions (Volynets *et al.*, 1992). The MA also contain clear unresorbed laths of plagioclase (up to ~0·6 mm in length) that grade continuously in size downward to the groundmass. These plagioclase laths are intermediate-to-calcic in composition (An_{45-67}; Table 2), and are compositionally similar to groundmass plagioclase within each sample (Tables 2 and 3). It is not clear, however, whether or not plagioclase was crystallizing with olivine and clinopyroxene before eruption.

The MA also contain crystals of Fe-rich orthopyroxene and sodic plagioclase which are not at equilibrium with the Mg-rich mafic phenocrysts. The Fe-rich orthopyroxene and sodic plagioclase in the MA are interpreted as xenocrysts, but they are of minor volumetric importance, and appear not to have affected the whole-rock compositions (see Table 3, and Volynets *et al.*, 1992).

INCOMPATIBLE ELEMENTS AND Sr–Nd–Pb ISOTOPES

Piip Series rocks show the incompatible element signature of arc volcanic rocks (Fig. 8), with high La/Sm (~3·3), Ba/La (~16), and Th/Ta (~3) compared with mid-ocean ridge

TABLE 1

Whole-rock major and trace elements

Series Name	*Komandor Series*											*Piip Series*				
Dredge no.	1	1	8	10	10	7	6	8	10	10	7	8	4	5	4	5	1
Rock type	*Basalts*		*Basaltic andesites*			*Andesites*							*Magnesian andesites*				
Sample	*2316/1*	*2316/2*	*35G8B*	*35-10/5*	*35G9E*	*35G7C*	*35G6B*	*35-8/1*	*35G9D*	*35-10/3*	*35G7A*	*35G8D*	*35-4/2*	*35-5/3*	*35G4X1*	*35-5/2*	*2316/4*
SiO_2	50·86	51·08	52·82	53·30	53·22	57·18	56·08	56·36	56·68	56·88	57·20	57·38	55·70	56·25	56·48	56·54	56·64
TiO_2	0·96	0·98	1·22	1·02	1·57	0·73	0·79	0·65	0·78	0·68	0·70	0·70	0·64	0·77	0·69	0·61	0·62
Al_2O_3	18·75	18·73	17·63	16·99	18·36	18·00	18·76	18·20	18·85	18·36	19·05	18·67	17·73	16·48	18·00	16·68	16·95
Fe_2O_3	1·65	1·62	2·37	2·80	4·16	0·93	1·71	1·63	1·63	1·63	1·30	1·15	1·39	0·98	1·23	1·28	1·25
FeO	4·48	4·60	4·29	4·18	3·02	3·72	3·66	3·23	3·73	3·25	3·46	3·60	3·83	4·09	4·09	3·69	4·02
MnO	0·14	0·14	0·14	0·11	0·05	0·13	0·12	0·08	0·16	0·10	0·09	0·10	0·05	0·11	0·14	0·12	0·11
MgO	5·20	5·66	5·08	4·76	4·48	3·40	4·28	4·38	4·08	4·04	3·80	3·86	6·18	6·40	6·14	6·62	5·74
CaO	11·09	10·69	11·24	8·74	9·24	7·24	6·90	7·20	7·14	7·48	6·68	6·90	8·66	7·22	7·00	7·20	7·18
Na_2O	3·58	3·58	3·40	3·86	3·70	3·76	3·52	4·05	4·02	4·05	3·76	3·52	3·65	3·46	3·40	3·89	3·58
K_2O	0·82	0·82	0·60	1·04	0·67	1·34	1·25	1·40	1·18	1·30	1·20	1·08	1·08	1·27	1·07	1·30	1·35
P_2O_5	0·22	0·22	0·13	0·13	0·19	0·14	0·11	0·11	0·17	0·11	0·14	0·12	0·14	0·18	0·15	0·13	0·15
H_2O^-	0·68	0·56	0·24	1·28	0·18	0·43	0·91	0·68	0·66	0·60	0·98	1·23	0·08	0·47	0·32	0·39	0·62
H_2O^+	1·18	1·26	0·53	1·14	0·37	1·72	1·90	1·66	1·31	1·66	1·66	1·81	1·14	1·83	0·94	1·37	1·86
Total	99·61	99·94	99·69	99·35	99·21	98·72	99·99	99·63	100·39	100·14	100·02	100·12	100·27	99·51	99·65	99·82	100·07
FeO*	5·96	6·06	6·42	6·70	6·76	4·56	5·20	4·70	5·20	4·72	4·63	4·63	5·08	4·97	5·20	4·84	5·14
FeO*/MgO	1·15	1·07	1·26	1·26	1·51	1·34	1·21	1·07	1·27	1·17	1·22	1·20	0·82	0·78	0·85	0·73	0·90
CaO/Al_2O_3	0·59	0·57	0·64	0·64	0·64	0·40	0·37	0·40	0·38	0·41	0·35	0·37	0·49	0·44	0·39	0·43	0·42
mg-no.	0·66	0·68	0·64	0·61	0·58	0·62	0·65	0·68	0·64	0·66	0·65	0·65	0·73	0·74	0·72	0·75	0·71
La	7·49	7·69	3·95	5·31	6·23	6·36	4·06		9·50		4·90	4·87			6·50		7·16
Ce	18·6	18·3	10·7	14·2	16·4	14·7	10·2		21·8		11·6	11·5			14·8		17·7
Nd	10·0	9·8		10·0	12·3	8·7			11·0		7·8						9·5
Sm	2·66	2·62	2·69	2·87	3·84	2·29	2·20		2·60		2·06	1·97			2·13		2·23
Eu	0·85	0·87	0·90	0·98	1·18	0·73	0·78		0·81		0·69	0·69			0·66		0·68
Tb	0·51	0·52	0·62	0·57	0·86	0·47	0·50		0·48		0·41	0·41			0·38		0·43
Yb	1·74	1·77	2·20	2·13	3·18	1·84	1·72		1·79		1·54	1·49			1·58		1·53
Lu	0·257	0·262	0·315	0·312	0·447	0·261	0·240		0·261		0·217	0·213			0·223		0·223
Y						18	19		20		19	20			19		
Sr	497	464	256	374	314	423	360		686		364	356			390		454
Ba	46	52	11	45	32	78	74		75		58	65			96		101
Rb						15	15		16		13	15			9		
Cs	0·16	0·17	0·24	0·21	0·16	0·20	0·17		0·27		0·21	0·18			0·14		0·15
U	0·27	0·24	0·09	0·38	0·13	0·26	0·17		0·30		0·24	0·20			0·39		0·45
Th	0·41	0·50	0·26	0·46	0·32	0·59	0·32		0·63		0·49	0·49			0·61		0·69
Hf	2·11	2·28	2·17	2·29	3·19	2·58	2·13		2·62		2·18	2·10			2·17		2·42
Ta	0·41	0·40	0·18	0·13	0·28	0·23	0·19		0·21		0·13	0·12			0·26		0·17
Co	26·3	28·4	25·6	28·4	24·4	17·3	21·9		17·8		17·3	17·0			21·9		23·1
Sc	26·5	26·5	29·3	28·4	27·9	19·3	20·7		17·5		18·3	18·4			19·7		17·2
Cr	636	590	236	219	110	39	32		52		61	64			167		564
Ni	62	57	52	31	33	27	22		33		29	27			64		132
La/Yb	4·3	4·3	1·8	2·5	2·0	3·5	2·4		5·3		3·2	3·3			4·1		4·7
Ba/La	6	7	3	8	5	12	18		8		12	13			15		14
Th/Ta	1·0	1·3	1·4	3·5	1·1	2·6	1·7		3·0		3·8	4·1			2·3		4·1

Series name	*Piip Series*																
Dredge no.	5	5	5	5	[1]	4	2	1	1	1	1	1	4	4	4	4	4
Rock name	*Magnesian andesites*				*Acid andesites*								*Dacites–rhyodacites*				
Sample	*35-5/5*	*35-5/1*	*35G5A*	*35G5B*	*2316/3*	*35G4X2*	*35G2A*	*35-1/2*	*35G1A*	*35-1/4*	*V36-1/6*	*35G1D*	*35-4/2*	*35G4A3*	*35G4A4*	*35G4A1*	*35G4A2*
SiO_2	56·96	57·12	58·00	58·06	59·58	58·23	61·02	61·85	63·20	64·02	64·78	65·50	67·50	68·28	68·38	68·64	69·12
TiO_2	0·77	0·73	0·67	0·66	0·52	0·53	0·54	0·51	0·48	0·42	0·44	0·37	0·35	0·41	0·43	0·43	0·47
Al_2O_3	16·02	16·21	17·19	17·28	17·81	18·30	18·34	16·58	17·89	16·17	16·21	17·62	15·80	16·05	15·95	16·00	16·30
Fe_2O_3	1·04	1·00	0·89	1·00	1·04	1·11	0·78	0·88	0·73	0·72	0·73	0·76	1·04	1·04	1·04	0·94	0·88
FeO	3·72	4·05	4·00	3·77	3·36	3·20	3·17	3·00	2·92	2·79	2·74	2·39	2·19	2·16	2·19	2·16	2·17
MnO	0·09	0·05	0·08	0·06	0·12	0·13	0·14	0·07	0·02	0·06	0·08	0·10	0·11	0·06	0·07		0·11
MgO	6·64	6·22	6·38	5·70	4·07	4·04	3·40	3·44	3·20	3·28	3·04	2·86	1·54	1·34	1·34	1·4	1·38
CaO	7·66	7·20	7·12	7·12	6·46	6·50	6·30	5·58	5·46	4·38	4·50	4·20	3·24	3·30	3·30	3·3	2·54
Na_2O	3·57	3·56	3·50	3·70	4·20	4·76	4·70	4·52	4·70	4·73	4·73	4·19	5·16	4·66	4·79	4·73	4·76
K_2O	1·20	1·30	0·96	1·08	1·50	1·66	1·02	1·25	1·20	1·35	1·35	1·08	1·82	1·55	1·00	1·6	1·50
P_2O_5	0·17	0·14	0·14	0·14	0·20	0·13	0·14	0·13	0·12	0·12	0·11	0·11	0·12	0·13	0·13	0·13	0·12
H_2O^-	0·23	0·86	0·50	0·36	0·54	0·26	0·19	0·30	0·18	0·40	0·34	0·16	0·51	0·24	0·24	0·20	0·30
H_2O^+	2·08	1·43	1·12	1·24	0·50	1·32	0·41	0·65	0·48	0·92	0·61	0·68	1·12	0·98	1·02	0·98	0·94
Total	100·15	99·87	100·55	100·17	99·90	100·17	100·15	98·76	100·58	99·36	99·66	100·02	100·50	100·20	100·38	100·51	100·59
FeO*	4·65	4·95	4·80	4·67	4·29	4·20	3·87	3·79	3·58	3·44	3·40	3·07	3·12	3·09	3·12	3·01	2·96
FeO*/MgO	0·70	0·80	0·75	0·82	1·06	1·04	1·14	1·10	1·12	1·05	1·12	1·07	2·03	2·31	2·33	2·15	2·15
CaO/Al_2O_3	0·48	0·44	0·41	0·41	0·36	0·36	0·34	0·34	0·31	0·27	0·28	0·24	0·21	0·21	0·21	0·21	0·16
mg-no.	0·76	0·74	0·75	0·73	0·68	0·68	0·66	0·67	0·67	0·68	0·67	0·67	0·54	0·49	0·49	0·51	0·51
La	6·48		6·27	6·34	7·83	7·00	8·02		8·01			7·96		10·1	9·31	9·62	8·66
Ce	16·2		15·1	15·0	17·7	16·0	18·7		17·2			17·5		21·8	20·9	21·2	18·9
Nd	8·5				8·8	9·0	9·5		8·6						10·3	10·7	
Sm	2·07		1·94	2·04	2·09	2·36	2·19		2·09			1·9		2·51	2·34	2·49	2·16
Eu	0·64		0·65	0·63	0·59	0·73	0·75		0·63			0·54		0·66	0·59	0·64	0·55
Tb	0·42		0·38	0·39	0·35	0·44	0·41		0·35			0·3		0·40	0·39	0·40	0·36
Yb	1·40		1·42	1·44	1·29	1·46	1·54		1·31			1·19		1·76	1·57	1·82	1·53
Lu	0·211		0·206	0·211	0·192	0·210	0·215		0·205			0·180		0·262	0·244	0·258	0·221
Y			18	18		17	17		17			16		19	18	18	18
Sr	392		384	376	548	532	429		487			490		321	307	325	304
Ba	93		87	96	137	132	137		137			166		208	184	207	176
Rb			9	6		13	7		8			9		11	10	14	13
Cs	0·14		0·12	0·13	0·18	0·17	0·19		0·19			0·21		0·27	0·28	0·27	0·24
U	0·29		0·28	0·19	0·41	0·39	0·43		0·51			0·53		0·65	0·64	0·66	0·58
Th	0·66		0·60	0·66	0·84	0·60	1·07		0·90			0·96		1·18	1·19	1·22	1·10
Hf	2·22		2·34	2·21	2·64	2·45	2·99		2·72			2·79		3·71	3·85	3·74	3·24
Ta	0·25		0·28	0·28	0·26	0·19	0·32		0·29			0·24		0·33	0·32	0·34	0·31
Co	24·6		25·4	19·9	18·7	15·9	14·4		14·6			12·1		7·9	7·0	7·1	6·8
Sc	17·4		18·1	16·7	12·5	14·1	14·2		13·8			9·3		7·9	7·0	7·3	6·6
Cr	468		262	241	312	47	19		60			42		13	11	12	10
Ni	123		127	89	79	53	20		35			58		10	8	11	10
La/Yb	4·6		4·4	4·4	6·1	4·8	5·2		6·1			6·7		5·7	5·9	5·3	5·7
Ba/La	14		14	15	17	19	17		17			21		21	20	22	20
Th/Ta	2·6		2·1	2·4	3·2	3·2	3·3		3·1			4·0		3·6	3·7	3·6	3·5

Major element analyses were performed at the Russian Institute of Volcanic Geology and Geochemistry, Petropavlovsk, Kamchatka, by wet chemistry, except Na_2O and K_2O (flame photometry). Trace elements (except Rb and Y) were analyzed by INAA at Cornell University. All samples were ground in an agate or Al-ceramic shatterbox. The INAA technique has been described by Kay *et al.* (1987), standard analyses by Kay & Kay (1988), and analytical precision by Romick *et al.* (1992). Rb and Y analyses by X-ray fluorescence were performed at the Institute of Geology and Geophysics, Novosibirsk, Siberia, Russia.

[1]Sampled by the Russian submersible *Mir*, Leg 23 of the 1990 cruise of the research vessel *Akademik Keldish*.

mg-no. = Mg/(Mg + Fe*), where $Fe^*/(Fe^{2+} + Fe^{3+}) = 0{\cdot}80$.

TABLE 2

Petrographic–mineralogic characteristics

Series name	*Rock name* (SiO_2)	*Sample(s)*	*Modal phenocrysts + xenocrysts* (%)	*Phenocrysts + xenocrysts (core comp.)*	*Groundmass (<0·1 mm) (silicate comp.)*
Piip Series	Magnesian andesites (55–58%)	Dredge 5	<8	olv (*mg*-no. 90·5–91·5) cpx (*mg*-no. 84–90) opx (*mg*-no. 67–69) plag (An_{39-50}) plag (An_{62-67}) ilm* (*mg*-no. 32–40)	olv (*mg*-no. 84–88) cpx (*mg*-no. 83–89) cpx (*mg*-no. 34–41) opx (*mg*-no. 84–88) plag (An_{60-65})
		2316/4	10–15	olv (*mg*-no. 87–89) cpx (*mg*-no. 84–87) plag (An_{65-68}) chrm† (*mg*-no. 51–64)	olv (*mg*-no. 84–86) cpx (*mg*-no. 80–84) plag (An_{56-65}) opx (*mg*-no. 78–82)
	Acid andesites (59–64%)	Dredges 1 and 2	25–35	opx (*mg*-no. 69–75) plag (An_{40-53}) plag (An_{83}) amph (*mg*-no. 68–72) cpx	opx (*mg*-no. 71–85) plag (An_{52-60}) cpx (*mg*-no. 77–82)
		2316/3	25–35	plag (An_{37-43}) plag (An_{67-70}) opx (*mg*-no. 68–72) amph (*mg*-no. 67–69) olv (*mg*-no. 87–89) cpx (*mg*-no. 87–88) cpx (*mg*-no. 77) chrm† (*mg*-no. 25–50) ilm* (*mg*-no. 14)	plag (An_{54-78}) cpx (*mg*-no. 77–86) opx (*mg*-no. 77–87)
	Dacites and rhyodacites (>63%)	Dredges 3 and 4	24–40	plag (An_{28-52}) plag (An_{66-84}) opx (*mg*-no. 64–67) amph (*mg*-no. 65–68) cpx (*mg*-no. 71) ilm* (*mg*-no. 12–13) mag* (*mg*-no. 7–10)	plag (An_{30-31}) opx (*mg*-no. 65–74) trydimite
Komandor Series	Basalts (<52%)	2316/1,2	5–10	olv (*mg*-no. 88–90) cpx (*mg*-no. 86–90) plag (An_{78-88}) chrm† (65–70)	plag (An_{31-51}) cpx (*mg*-no. 72–87)
	Basaltic andesites (52–55%)	Dredges 6–9	10–30	olv cpx plag	cpx plag
	Andesites (55–58%)	Dredges 6–9	25–35	plag (An_{76-83}) cpx (*mg*-no. 84–87) olv (*mg*-no. 84)	plag (An_{41-45}) cpx (*mg*-no. 68–81)

Summary of data from Romick *et al.* (in press), and Volynets *et al.* (1992).

Abbreviations: olv, olivine; cpx, clinopyroxene; opx, orthopyroxene; plag, plagioclase; amph, amphibole; chrm, chromian spinel; ilm, ilmenite; mag, magnetite.

*Inclusions in orthopyroxene phenocrysts/xenocrysts.

†Inclusions in olivine phenocrysts/xenocrysts.

basalt (MORB). This signature is not, however, as strongly developed as in volcanic rocks of the Central and Eastern Aleutians. For example, K/La in the Piip Series is within the range of Aleutian basalts, but Ba/La, Th/La, and Th/Ta are broadly transitional toward MORB (Fig. 9). Cs, K, and Sr spikes on MORB-normalized incompatible element diagrams, and

TABLE 3

Modal analyses of magnesian andesites (vol. % based on ~1200 points)

Sample	*Phenocrysts**	*Xenocrysts*
V35G5A	2–3% olivine <1% clinopyroxene	1–2% orthopyroxene 2% plagioclase
V35G5B	1% olivine <1% clinopyroxene	1% orthopyroxene 1–2% plagioclase
2316/4	3–4% olivine 2–3% clinopyroxene	1% orthopyroxene

*All magnesian andesites also contain clear, unresorbed laths of plagioclase that grade continuously in size from groundmass to subphenocrysts and phenocrysts (up to 0·6 mm). (See Table 2 for compositions and text for discussion.)

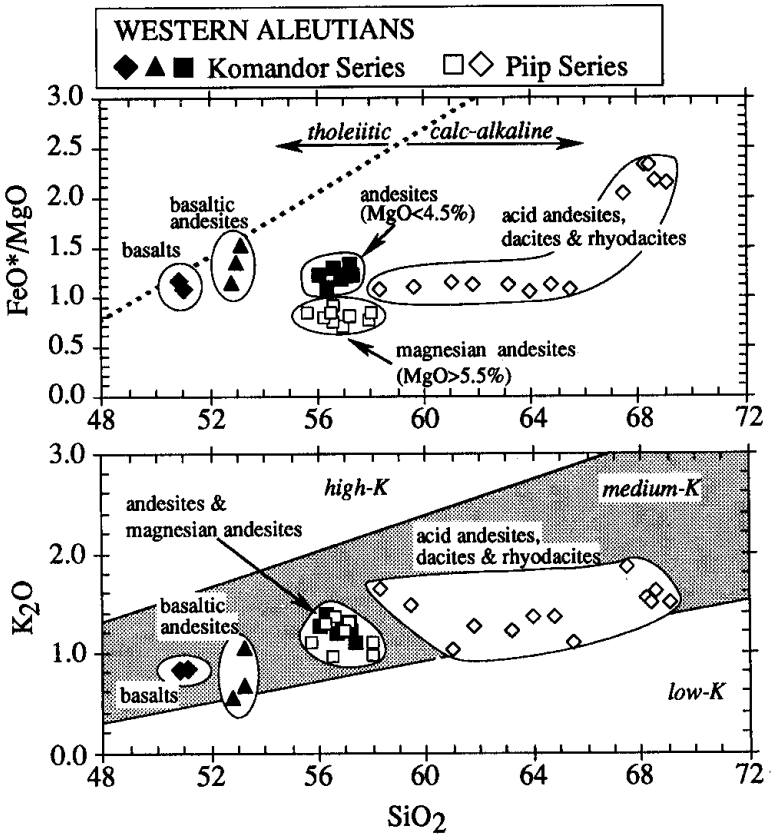

FIG. 4. FeO*/MgO and K_2O vs. SiO_2 for volcanic rocks of the Piip and Komandor Series (see text). Calc-alkaline–tholeiitic boundary line is from Miyashiro (1974). Rock names and symbols in this figure are used throughout this paper.

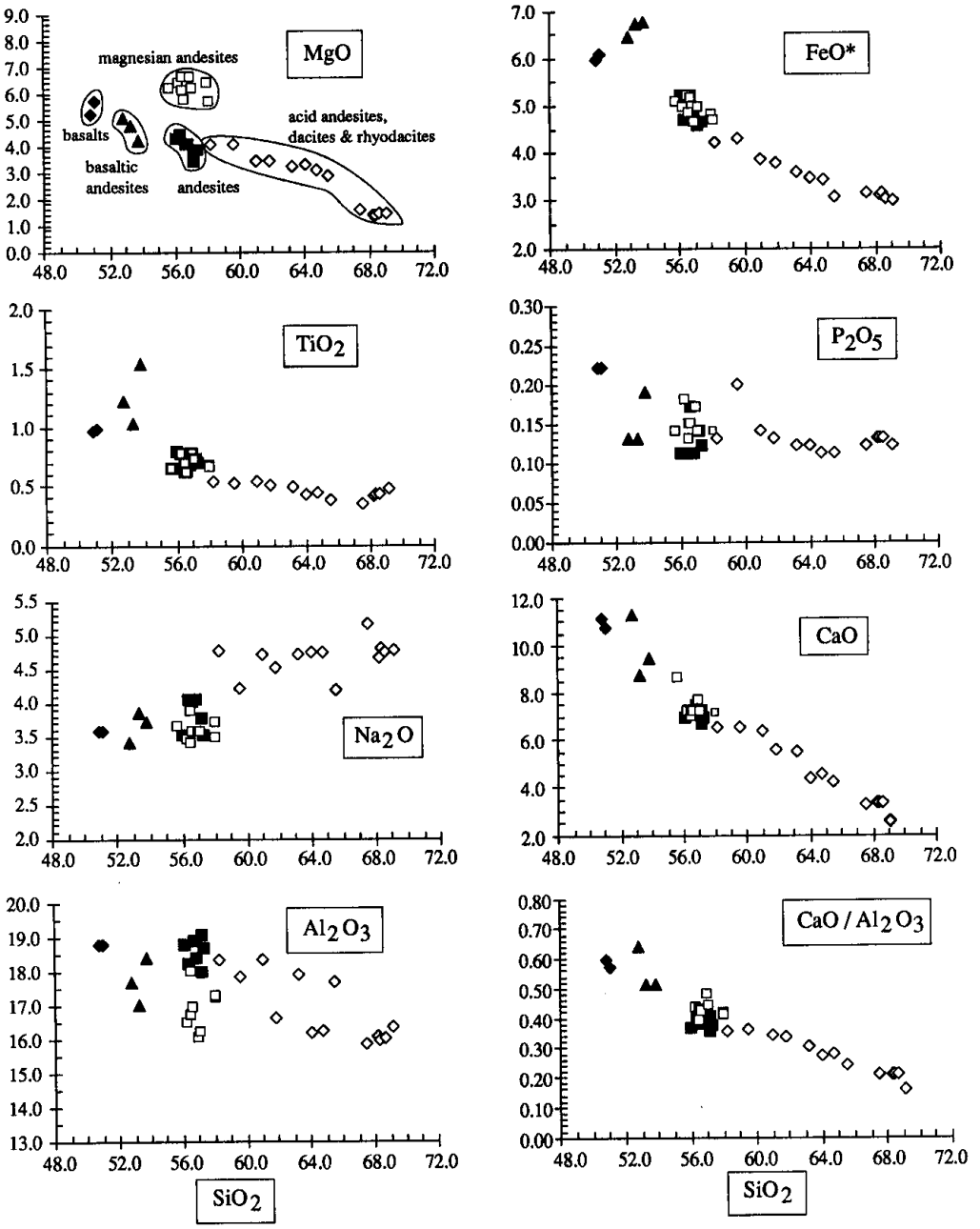

FIG. 5. Major element variation in Piip and Komandor Series rocks. Rock names and symbols are the same as in Fig. 4.

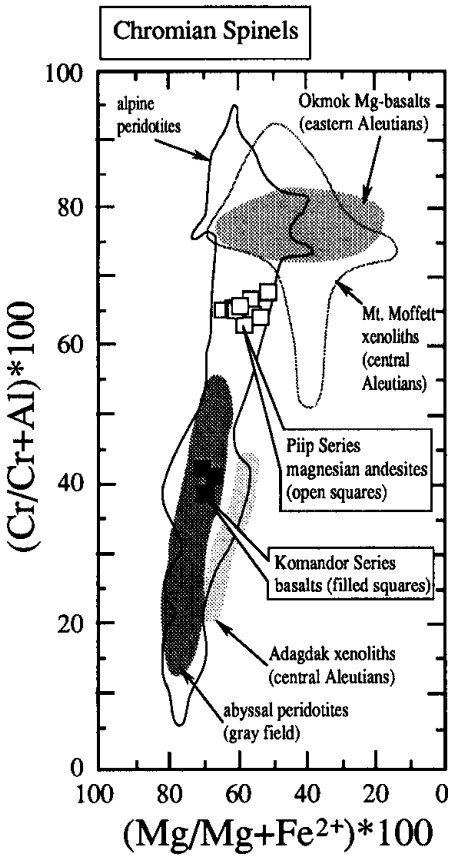

FIG. 6. Chromian spinel inclusions in olivine phenocrysts in Piip Series MA and Komandor Series basalts. The figure is modified from Dick & Bullen (1984). It should be noted that chromite inclusions in the Piip Series magnesian andesites are more Cr rich than those in Komandor Series basalts, and abyssal peridotites. Chromite inclusions in the MA are more similar to those in other Aleutian lavas' xenoliths and in alpine peridotites (discussion in text). Fields for Okmok Mg-basalts are from Nye & Reid (1986), Mt. Moffett xenoliths from Conrad & Kay (1984), Adagdak xenoliths from DeBari *et al.* (1987), and abyssal and alpine-type peridotites from Dick & Bullen (1984).

low relative concentrations of Ta and Ti (Fig. 10D) are also distinctly arc-like, but ratios among the alkali and alkaline earth elements (e.g., Rb/Cs, K/Rb, and K/Ba) are more characteristic of MORB (Fig. 11). Concentrations of the incompatible elements in Piip Series rocks generally increase from MA to rhyodacite, but interelement ratios are similar at all silica levels (Figs. 8 and 9).

Komandor Series basalts and basaltic andesites also show spikes at Cs, K, and Sr, but otherwise show a broad range of interelement ratios that resemble those of enriched and normal MORB, respectively (Figs. 8 and 10). It should be noted that Cs, K, and Sr enrichment in these rocks appears in the absence of discernible Ta or Ti depletion (Fig. 10). Andesites of the Komandor Series have incompatible element characteristics similar to those of the Piip Series rocks (Figs. 8–10), but some have flatter REE patterns, with higher relative Ta concentrations (e.g., sample 35G6B, Fig. 8B).

The presence of a subduction component in the Western Aleutian rocks is implied by Cs, K, and Sr spikes on normalized incompatible element plots, and by low ratios of high field

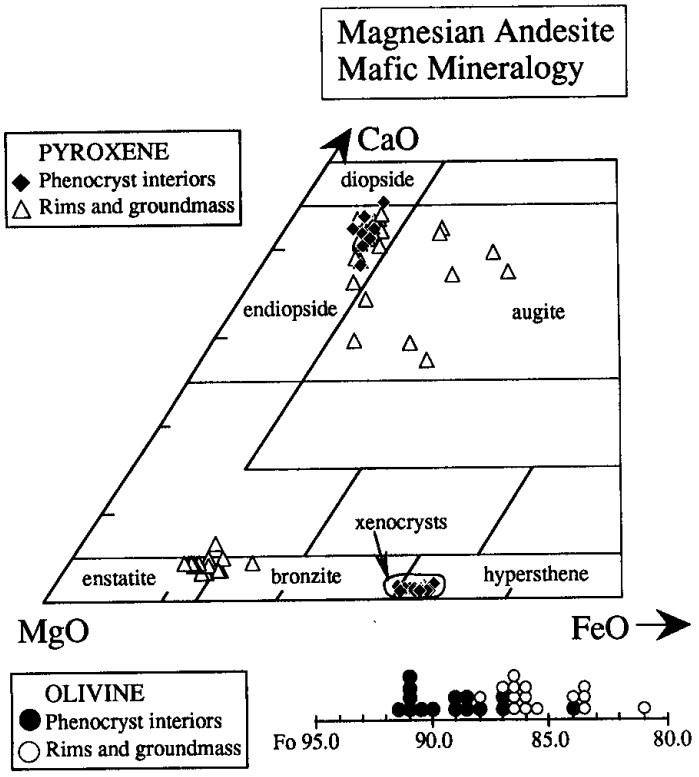

FIG. 7. Mafic mineralogy in Piip Series MA. It should be noted that the olivine and clinopyroxene phenocrysts together with groundmass pyroxene form a primitive assemblage, consistent with derivation from a mantle source. Fe-rich orthopyroxenes (hypersthene), which are similar to those in Piip Series dacites (Romick *et al*,. in press), are interpreted as xenocrysts. Data are from Volynets *et al.* (1992) and unpublished results.

strength to rare earth elements (low HFSE–REE ratios). Normally this signature is accompanied by Pb, Sr, and Nd isotopic ratios that are distinct from those of MORB, but in the Piip and Komandor Series, the isotopic signature is broadly MORB-like. This is clearest in Fig. 12, which shows that Pb isotopes in the Western Aleutian rocks are very nonradiogenic, with $^{206}Pb/^{204}Pb$ ratios ($<18{\cdot}2$) lower than nearly all of North Pacific MORB [note that, in Fig. 12, one North Pacific MORB analysis has $^{206}Pb/^{204}Pb = 18{\cdot}16$: sample A1407-B1 from White *et al.* (1987)]. With respect to Pb isotopes, the Piip and Komandor Series rocks are more similar to basalts of some Western Pacific marginal basins (e.g., Hickey-Vargas, 1991; Tatsumoto & Nakamura, 1991) than to North Pacific MORB (Fig. 12). Nd and Sr isotopes are also broadly MORB-like (Table 4; see also Romick *et al.*, in press). In Piip Series rocks ε_{Nd} falls in a narrow range (10·0–10·6), and is only slightly more variable for the Komandor Series ($\varepsilon_{Nd} = 10{\cdot}0$–$11{\cdot}3$; Fig. 13). The total range of $^{87}Sr/^{86}Sr$ ratios is 0·70255–0·70281, with the lowest values in the Komandor Series basalts and basaltic andesites (0·70255–0·70260), higher values in the andesites (0·70257–0·70273), and the highest values in the MA and silicic rocks of the Piip Series (0·70262–0·70281). $^{87}Sr/^{86}Sr$ in the Piip and Komandor Series rocks is thus relatively variable and high compared with ε_{Nd} (Fig. 13).

Among volcanic rocks of the modern Central and Eastern Aleutian arc, only the Adak-type MA, or Aleutian adakites (Defant & Drummond, 1990) are as isotopically MORB-like as the Western Aleutian suite (see Kay, 1978). Adakites were originally sampled on Adak

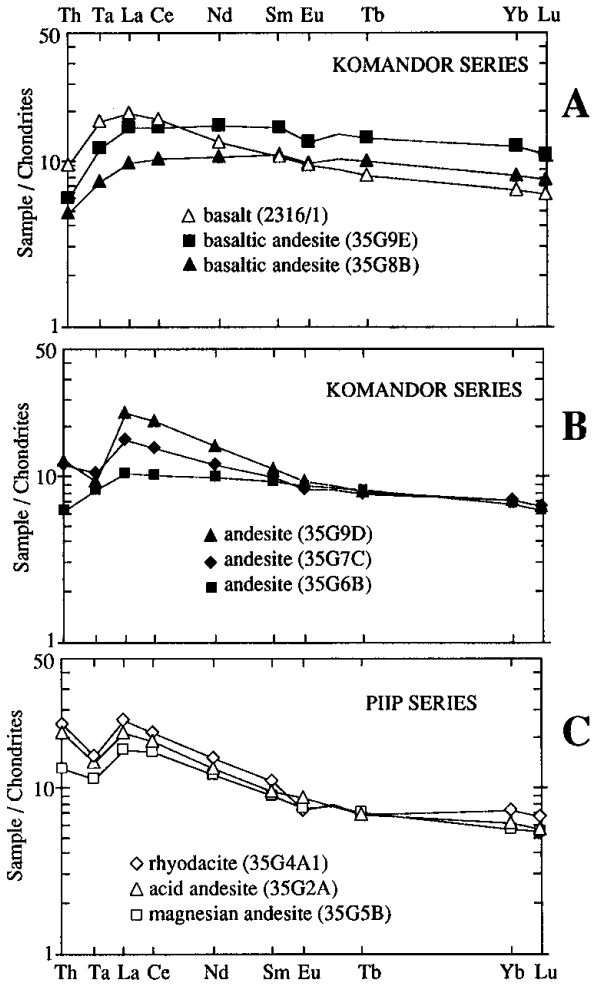

FIG. 8. Chondrite-normalized REE, Th, and Ta in Komandor and Piip Series rocks. In (A), the depleted patterns of the basaltic andesites compared with the basalts should be noted. In (B) it can be seen that rocks of andesitic composition range from flat patterns such as those for the basaltic andesites, to LREE-enriched patterns with low relative Ta, similar to rocks of the Piip Series (C), which have approximately parallel patterns from MA to rhyodacite. Data are from Table 1. Normalizing values are Leedy chondrite: Th (0·050), Ta (0·022), La (0·378), Ce (0·976), Nd (0·716), Sm (0·230), Eu (0·0866), Tb (0·0589), Yb (0·249), Lu (0·0387).

Island in the Central Aleutians (sample ADK53; Kay, 1978), but they have also been dredged from the far western arc, at the Aleutian–Kamchatka junction (sample 70B49; Scholl *et al.*, 1976; Kay, 1978). All Aleutian adakites have high Sr concentrations (>1500 ppm), high large ion lithophile (LILE) and light REE concentrations (LREE), and highly fractionated REE patterns that require residual garnet in the source (Fig. 14). Isotopic and interelement ratios among the alkali and alkaline-earth elements in Aleutian adakites are broadly MORB-like. It should be noted in particular that the Western Aleutian adakite of Kay (1978) has less radiogenic Pb ($^{206}Pb/^{204}Pb < 17{\cdot}9$) than even the Piip and Komandor Series rocks (Fig. 12). Kay (1978) concluded that Aleutian adakites formed as small percentage melts of the subducting slab, which interacted with the mantle wedge as they rose to the surface. Although Piip Series MA have major element and isotopic characteristics broadly similar to

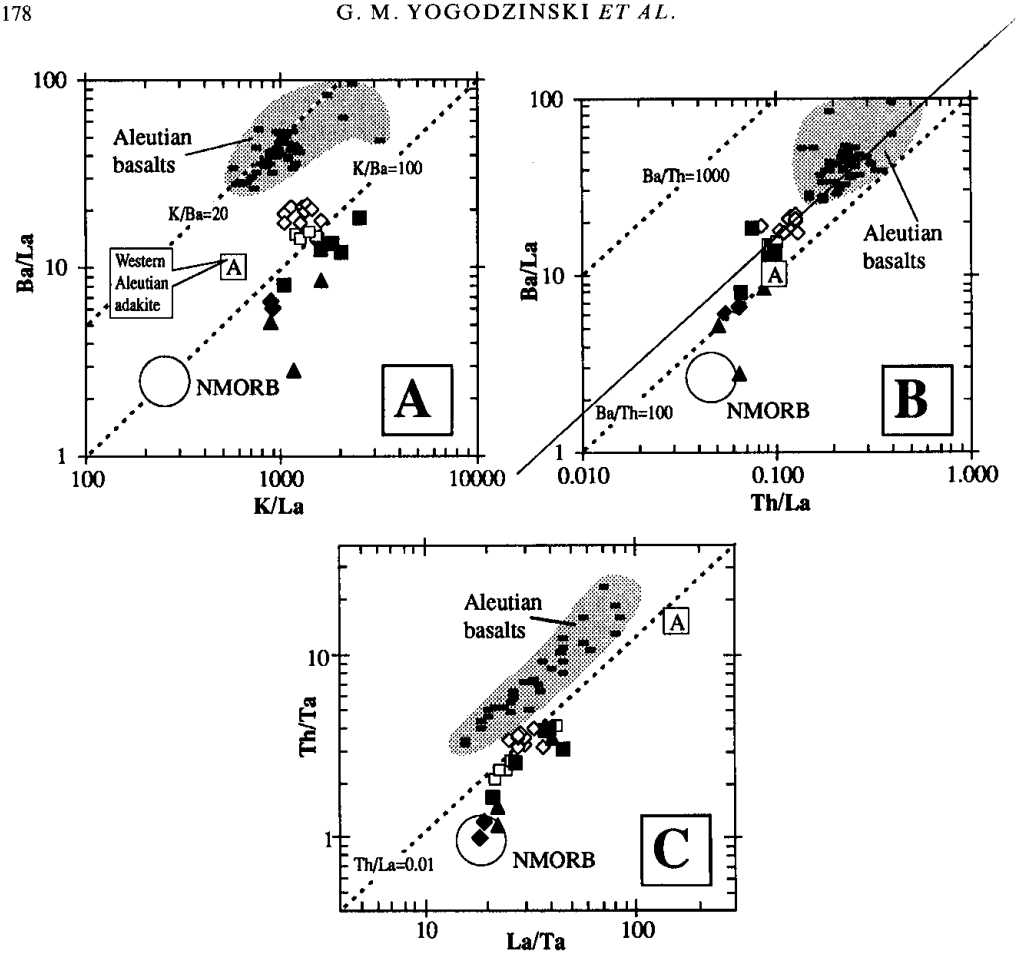

FIG. 9. Incompatible element ratios in the Western Aleutian rocks (Table 1, symbols as in Fig. 4) compared with basalts of the Central and Eastern Aleutians and NMORB. Western Aleutian adakite is average value from Yogodzinski *et al.* (in prep.). In (A), the Western Aleutian rocks have K/La as high as or higher than those for average Aleutian basalts, but Ba/La ranges from NMORB up to only 15–20, well below those of average Aleutian basalts (Ba/La of 30–40). In (B), the similarity in behavior of Ba and Th in all the Aleutian rocks, and the continuous variation in Ba/La and Th/La between NMORB and the reference Aleutian basalts should be noted. In (C), the continuous variation between NMORB and Aleutian basalts should be noted. Aleutian basalt data are from Kay & Kay (in press), and NMORB from Sun & McDonough (1989) are listed in Fig. 10 caption.

Aleutian adakite, it is an important point that these primitive andesitic rocks are readily distinguished by their incompatible element characteristics, and that they each appear to have analogs in other arcs (e.g., Baja and Japan; see Fig. 14).

ORIGIN OF THE WESTERN ALEUTIAN SUITE

The subduction component: a slab-melting origin

The presence of an arc trace element signature is consistent with the calc-alkaline affinity of most Piip and Komandor Series rocks (Fig. 4), and with the crystal-rich texture and mineralogy of the evolved samples (acid andesites to rhyodacites). Exceptions are basalts and basaltic andesites of the Komandor Series, which lack some aspects of the arc trace element signature (e.g., high Th/Ta) and are transitional between the calc-alkaline and

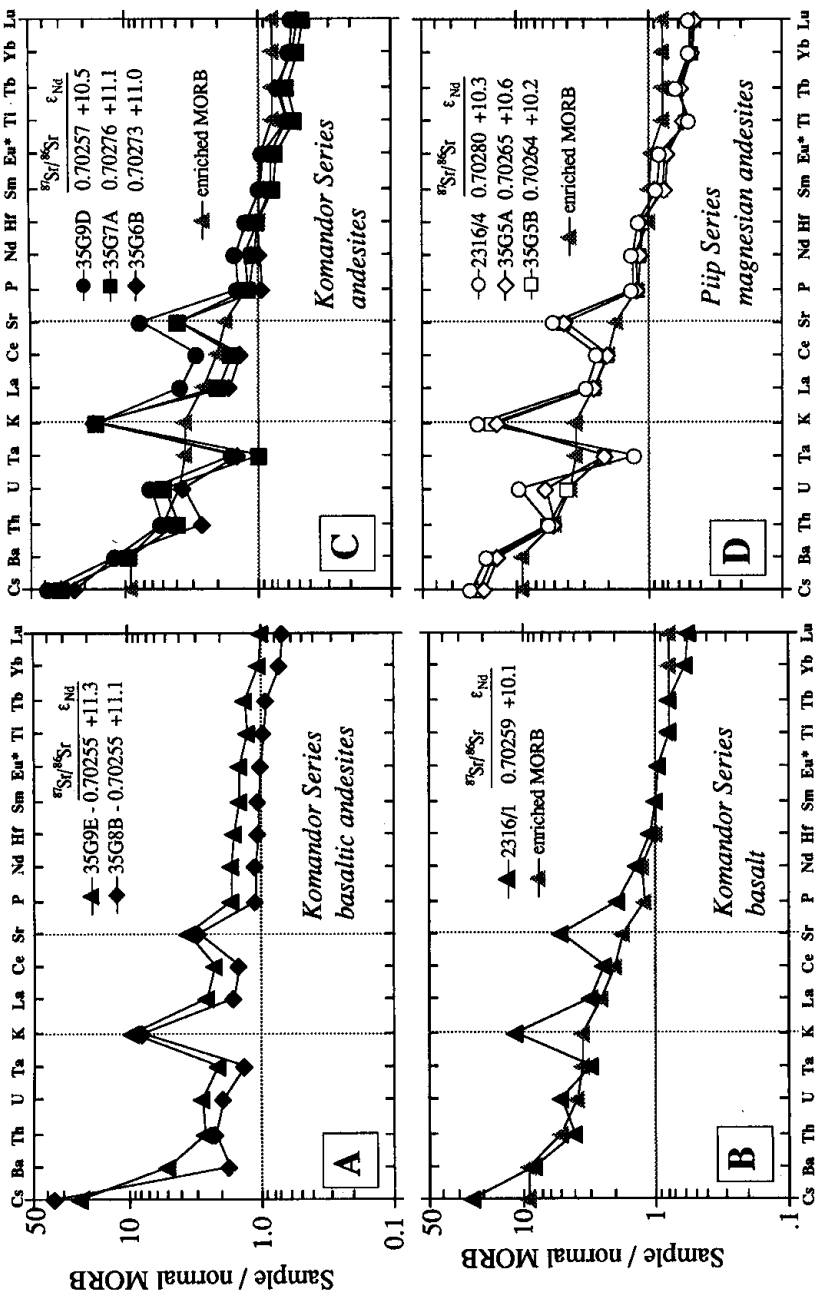

FIG. 10. Incompatible elements in Piip and Komandor Series rocks normalized to NMORB. It should be noted that all of the Western Aleutian rocks have prominent spikes in Sr, K, and Cs which are a factor of 2–4 above the baseline given by the REE. This Sr enrichment is similar to that in volcanic rocks of the Central and Eastern Aleutian arc (fig. 14 of Kay & Kay, in press). In (A) and (B), the similarity in REE and HFSE of the basaltic andesites to NMORB, and of the basalts to enriched MORB, is noteworthy. Also, the pattern formed by these elements in the basalts and basaltic andesites is smooth compared with those in the andesites and Piip Series MA [(C) and (D)], which clearly have low Ta and Ti relative to the REE (i.e., low Ta/La and Ti/Tb in the andesites and MA). Plotting order and normalizing values from Sun & McDonough (1989) are Lu (0·455), Yb (3·05), Tb (0·670), Ti (7600), Eu* (1·02), Sm (2·63), Hf (2·05), Nd (7·30), P (510), Sr (90), Ce (7·50), La (2·50), K (600), Ta (0·132), U (0·047), Th (0·120), Ba (6·30), and Cs (0·007).

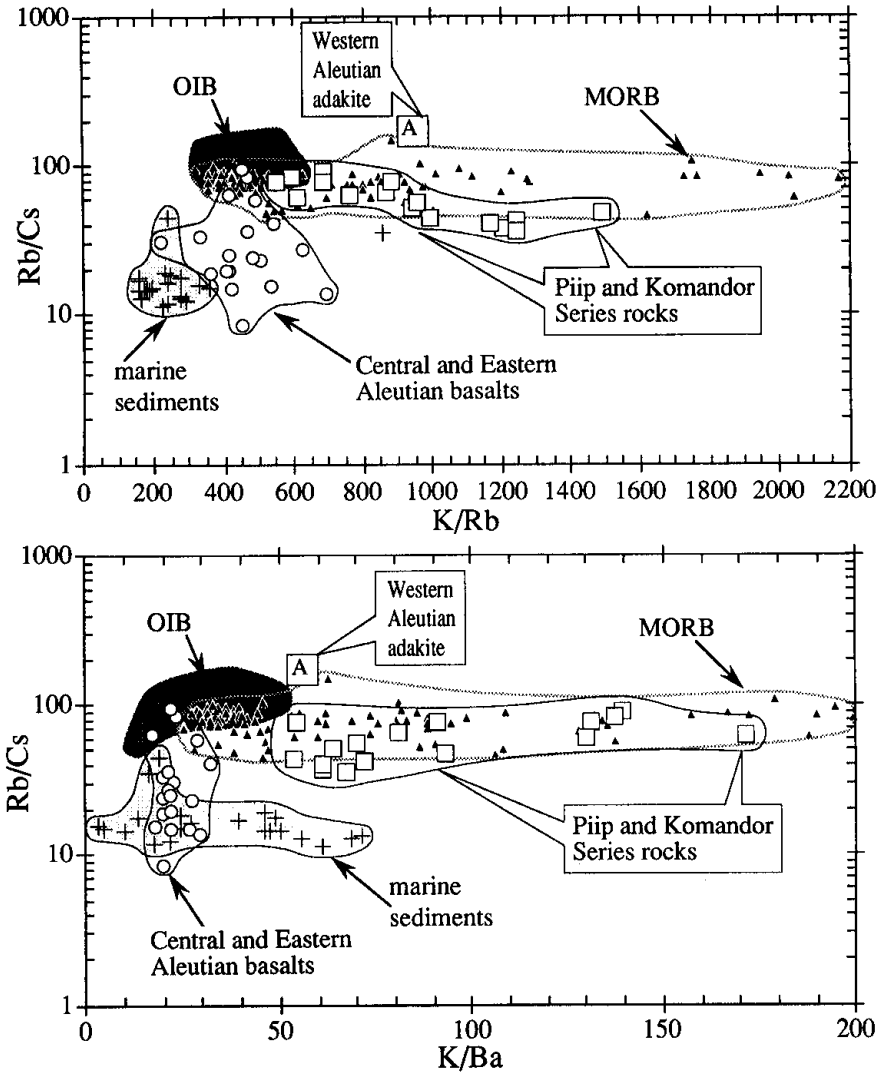

FIG. 11. Alkali element ratios in Western Aleutian rocks (Table 4) compared with those of MORB, OIB, marine sediment, and basalts from the Central and Eastern Aleutians. This figure is similar to fig. 1 of Hart & Reid (1991). Western Aleutian adakite is average value from Yogodzinski *et al.* (in prep.). The similarity of the Western Aleutian rocks to NMORB, consistent with Pb, Sr, and Nd isotope ratios, is noteworthy (see also Table 3 and Figs. 12–14). MORB (small triangles) and OIB (dark field) are from Morris & Hart (1983) and Hofmann & White (1983). Data considered 'suspect' by Hofmann & White (in parentheses in their table 1) are excluded from this figure. Marine sediment data were referenced in fig. 1 of Hart & Reid (1991). Aleutian basalt data are from Kay & Kay (in press) and references therein.

tholeiitic trends (Fig. 4). In all cases, however, the MORB-like isotopic characteristics of the Western Aleutian rocks require that the subduction component originated largely in the basalt–gabbro portion of subducting oceanic crust, which was hydrothermally altered to produce modest deviations from normal MORB in some mobile elements (e.g., high $^{87}Sr/^{86}Sr$ relative to ε_{Nd}). Components from marine sediment appear to be absent. In a simple mixing–melting model (Fig. 15), Western Aleutian adakite provides an endmember

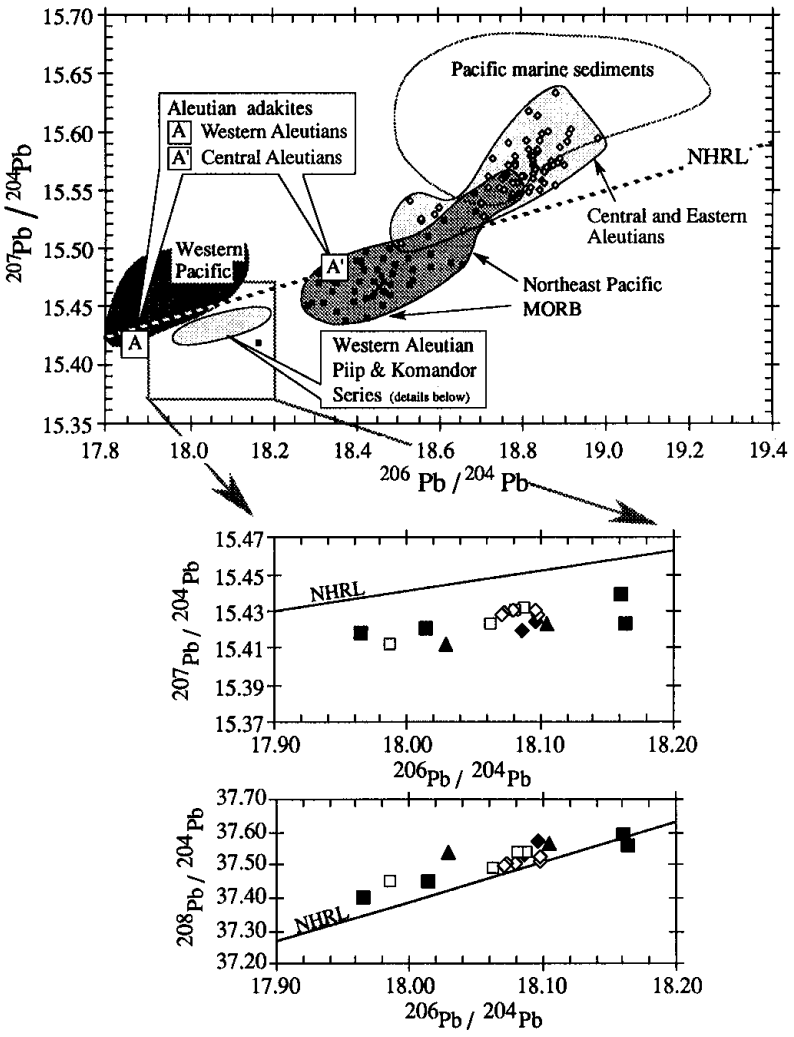

FIG. 12. Pb isotopes in Western Aleutian rocks (Table 4, symbols as in Fig. 4). The non-radiogenic Pb isotopes in Piip and Komandor Series rocks compared with Northeast Pacific MORB (Juan de Fuca and Gorda ridge) should be noted. The Western Aleutian data are at the nonradiogenic limit of MORB throughout the Pacific (see White *et al.*, 1987), but have low $^{206}Pb/^{204}Pb$ similar to some marginal basin basalts of the Western Pacific. Aleutian adakite sample 'A' is from the Western Aleutians, and 'A" is from Adak Island in the Central Aleutians [samples 70B49 and ADK53, respectively, of Kay (1978)]. Pacific marine sediment and MORB data sources were referenced in fig. 9 of Yogodzinski *et al.* (1993). Cental and Eastern Aleutian data were referenced in Kay & Kay (in press). Western Pacific field is a subset of Tertiary age marginal basin basalts from Hickey-Vargas (1991). NHRL is the northern hemisphere reference line of Hart (1984).

composition that reproduces many of the incompatible element and isotopic characteristics of Piip and Komandor Series rocks when mixed with depleted MORB mantle.

Isotopic and alkali element data imply that components from marine sediment are not present in the Western Aleutian rocks. Pb isotopes in the Western Aleutian rocks define a narrow field that parallels the northern hemisphere reference line at the non-radiogenic limit of Pacific MORB. Low $^{207}Pb/^{204}Pb$ indicates that Pb in the Western Aleutian rocks has not been recycled from marine sediment. High Rb/Cs, K/Rb, and K/Ba in the Western Aleutian

TABLE 4

Isotopes

	$^{206}Pb/^{204}Pb$	$^{207}Pb/^{204}Pb$	$^{208}Pb/^{204}Pb$	$^{87}Sr/^{86}Sr$	$^{143}Nd/^{144}Nd$	ε_{Nd}
			Basalts			
2316/1	18·096	15·424	37·570	0·70259	0·513109	10·05
2316/2	18·087	15·419	37·532	0·70260	0·513105	9·98
			Basaltic andesites			
V35/G9E	18·106	15·423	37·561	0·70255	0·513173	11·30
V35/G8B	18·030	15·411	37·537	0·70255	0·513163	11·11
			Andesites			
V35/G9D	18·165	15·422	37·560	0·70257	0·513131	10·48
V35/G7C	18·161	15·438	37·594	0·70269	0·513129	10·44
V35/G7A	18·015	15·420	37·449	0·70276	0·513165	11·15
V35/G6B	17·966	15·418	37·397	0·70273	0·513158	11·01
			Magnesian andesites			
2316/4	17·987	15·412	37·448	0·70280	0·513121	10·29
V35/G5B	18·089	15·431	37·535	0·70264	0·513116	10·19
V35/G5A	18·082	15·430	37·539	0·70265	0·513139	10·64
V35/G4X1	18·063	15·422	37·487	0·70269	0·513139	10·64
			Acid andesites			
V35/G2A	18·099	15·427	37·509	0·70266	0·513124	10·35
V35/G1A	18·098	15·430	37·520	0·70262	0·513112	10·11
2316/3	18·072	15·428	37·498	0·70271		
			Rhyodacites			
V35/G4A1	18·081	15·430	37·500	0·70276	0·513122	10·31
V35/G4A2	18·074	15·429	37·503	0·70278	0·513129	10·44

All isotope analyses were by thermal ionization mass spectrometry at Cornell University. Mean standard values and analytical precision (±2 SD) reported below are based on analyses performed between August and November 1990.

Analytical technique for Pb was according to White *et al.* (1990). Measured values for NBS SRM-981 Pb standard were $^{206}Pb/^{204}Pb = 16{\cdot}907$, $^{207}Pb/^{204}Pb = 15{\cdot}435$, and $^{208}Pb/^{204}Pb = 36{\cdot}496$. Each ratio was corrected for mass fractionation independently assuming standard values of $^{206}Pb/^{204}Pb = 16{\cdot}937$, $^{207}Pb/^{204}Pb = 15{\cdot}493$, and $^{208}Pb/^{204}Pb = 36{\cdot}705$. Analytical precision of ±0·008 ($^{206}Pb/^{204}Pb$), ±0·007 ($^{207}Pb/^{204}Pb$), and ±0·024 ($^{208}Pb/^{204}Pb$) was based on 13 analyses of NBS SRM-981. Nd analyses were performed on Ta single filaments after Walker *et al.* (1989) by quintuple collector dynamic procedure. Ratios were corrected for mass fractionation assuming $^{146}Nd/^{144}Nd = 0{\cdot}7219$. Measured values for La Jolla Nd standard were $^{143}Nd/^{144}Nd = 0{\cdot}511817 \pm 0{\cdot}000012$ and $^{145}Nd/^{144}Nd = 0{\cdot}348412 \pm 0{\cdot}000013$, based on 15 analyses. ε_{Nd} values are deviations in 10^4 from present-day chondritic $^{143}Nd/^{144}Nd$ assuming La Jolla $\varepsilon_{Nd} = -15{\cdot}15$ (Lugmair & Carlson, 1978; Wasserburg *et al.*, 1981). Sr analyses were carried out on W single filaments by quadruple collector dynamic procedure. Ratios were corrected for mass fractionation assuming $^{86}Sr/^{88}Sr = 0{\cdot}11940$. Average measured value for NBS SRM-987 Sr standard was $^{87}Sr/^{86}Sr = 0{\cdot}710228$, with analytical precision of ±0·000042, based on 28 analyses.

rocks are similarly MORB-like, and appear to exclude not only marine sediment, but also OIB-type mantle (ocean island basalt) as the principal source of these components (Fig. 11). Finally, low $^{87}Sr/^{86}Sr$ (0·70255–0·70281) implies that Sr spikes in Western Aleutian rocks cannot be due in a large part to recycling from Pacific marine sediment with high $^{87}Sr/^{86}Sr$. Using the REE as a baseline and the plotting order of Sun & McDonough (1989), Sr concentrations in the Western Aleutian rocks are 2–3 times greater than expected from normal incompatible element behavior (Sr in Fig. 10 does not fall on a straight line between Ce and Nd). Under these constraints, only 4–5% (certainly not 40–60%) of the Sr budget in the Western Aleutian rocks can have originated in a radiogenic source. In any simple mixture, the combined alkali element and isotopic data limit to near zero the portion of subducted components in Western Aleutian rocks that can have originated in marine sediment.

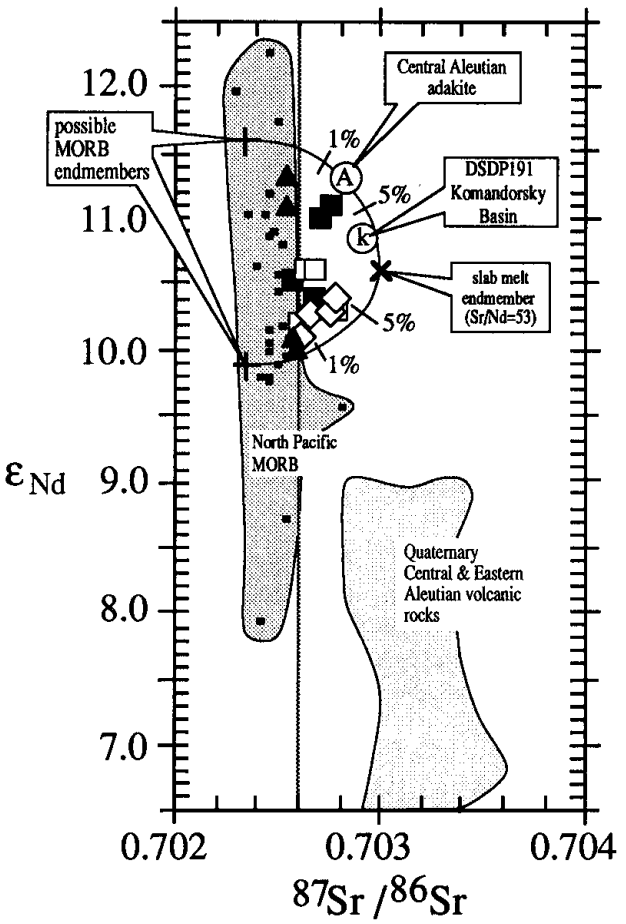

FIG. 13. ε_{Nd} vs. $^{87}Sr/^{86}Sr$. Piip and Komandor Series rocks (symbols as in Fig. 4) and Komandorsky Basin basalt (DSDP191) have ε_{Nd} similar to prevalent North Pacific MORB (gray field surrounding small filled squares). The high $^{87}Sr/^{86}Sr$ compared with ε_{Nd} in the Piip and Komandor Series rocks should be noted. Mixing lines between possible MORB peridotite endmembers (2 ppm Nd, 25 ppm Sr) and hypothetical slab melt with Sr and Nd concentrations similar to adakite (Kay, 1978; Yogodzinski *et al.*, in prep.), and $^{87}Sr/^{86}Sr$ for slightly altered oceanic crust (~0·703) encompass the Western Aleutian data at 1–5% mixture of slab melt. North Pacific MORB data sources (Juan de Fuca and Gorda ridges) were referenced in Fig. 8 of Yogodzinski *et al.* (1993). Quaternary Central and Eastern Aleutian data were referenced in Kay & Kay (in press). DSDP191 and adakite analyses are from Kay *et al.* (1986).

We conclude that the Western Aleutian rocks were derived from a mixture of two isotopically MORB-like sources: (1) the subducting oceanic crust, and (2) the overlying mantle wedge. The only non-MORB isotopic characteristic in the Western Aleutian rocks is elevated $^{87}Sr/^{86}Sr$ compared with ε_{Nd} (Fig. 13). This kind of isotopic shift is commonly attributed to the alteration of the mantle wedge by metasomatic fluids derived from the dewatering of subducting oceanic crust (e.g., Ellam & Hawkesworth, 1988; Stern *et al.*, 1991). It is presumed that such fluids are Sr enriched, with high Sr/Nd, and that they readily alter the Sr but not the Nd characteristics of the mantle wedge. Simple trace element models indicate, however, that small percentage melting of subducting (eclogitic) oceanic crust will also produce melts that have high Sr concentrations as well as high Sr/Nd (e.g., Kay, 1978). If the slab has undergone seawater alteration to give it high $^{87}Sr/^{86}Sr$ relative to ε_{Nd}, the mixing

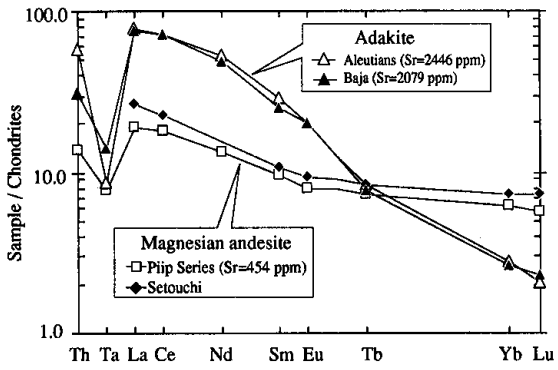

FIG. 14. Chondrite-normalized REE, Th, and Ta of Piip Series magnesian andesite (sample 2316/4, Table 1) compared with other magnesian andesites including adakites: Western Aleutian adakite [sample V3842Y3 from Yogodzinski *et al.* (in prep.)], Setouchi magnesian andesite [sample SD264 from Tatsumi & Ishizaka (1982)], and Baja adakite [sample J.1.1 from Saunders *et al.* (1987)]. Normalizing values are as in Fig. 8.

of a slab melt into the mantle wedge will produce the same effect as a hypothetical metasomatic fluid. A general model of this kind is shown in Fig. 13. In the Western Aleutians, a mixture of adakite (hypothetical slab melts) with prevalent North Pacific MORB will similarly reproduce the low Pb isotope ratios of the Piip and Komandor Series rocks (Fig. 12).

A more general application of a slab melt + mantle wedge model (Fig. 15) demonstrates that mixing 4% Western Aleutian adakite (model slab melt) into 96% depleted MORB mantle produces a peridotite with incompatible element characteristics like those of many of the Western Aleutian rocks. Batch melting of this enriched source produces a magma with incompatible element concentrations and interelement ratios similar to those of the Piip Series MA and/or andesites of the Komandor Series. It is unlikely that the Piip Series MA have formed by simple batch melting processes (see below), but Fig. 15 demonstrates that mixtures of hypothetical mantle wedge and slab melt endmembers are a reasonable means of producing the subduction trace element signature in a peridotite source.

The presence of excess Cs in the MA compared with the simple model (Fig. 15), combined with the Pb isotope data, indicates that the Piip lavas do not contain Pb from marine sediment, but may contain a small amount of Cs from this source. This means that Cs and Pb, which are both good tracers of sediment, may have been substantially decoupled in the genesis of the Piip rocks. In this regard, light elements such as Be and B are of interest, because they are perhaps the most sensitive tracers of sediment available (Morris *et al.*, 1990). Preliminary data indicate that Be from marine sediment may be present in the only Piip sample that has been analyzed ($2{\cdot}7 \times 10^6$ atoms/g ^{10}Be in a Piip dacite; J. Morris & F. Tera, pers. comm., 1993). We emphasize, however, that without more complete Be data (i.e., ^{9}Be/^{10}Be, and a high leachate analysis) the origin of this apparently high ^{10}Be concentration cannot be firmly established.

The model in Fig. 15 is similar to that proposed by Kay (1978), and it supports the general idea that adakite is an important mixing endmember in Aleutian magma genesis (e.g., Kay, 1980). The key element of this model is the highly fractionated incompatible element pattern of Aleutian adakite. We repeat that the LILE, REE, and isotopic characteristics of Aleutian adakite are consistent with 3–5% melting of an eclogitic MORB source (Kay, 1978). In addition, the extreme HSFE depletion in adakite suggests that rutile or some other Ti-rich

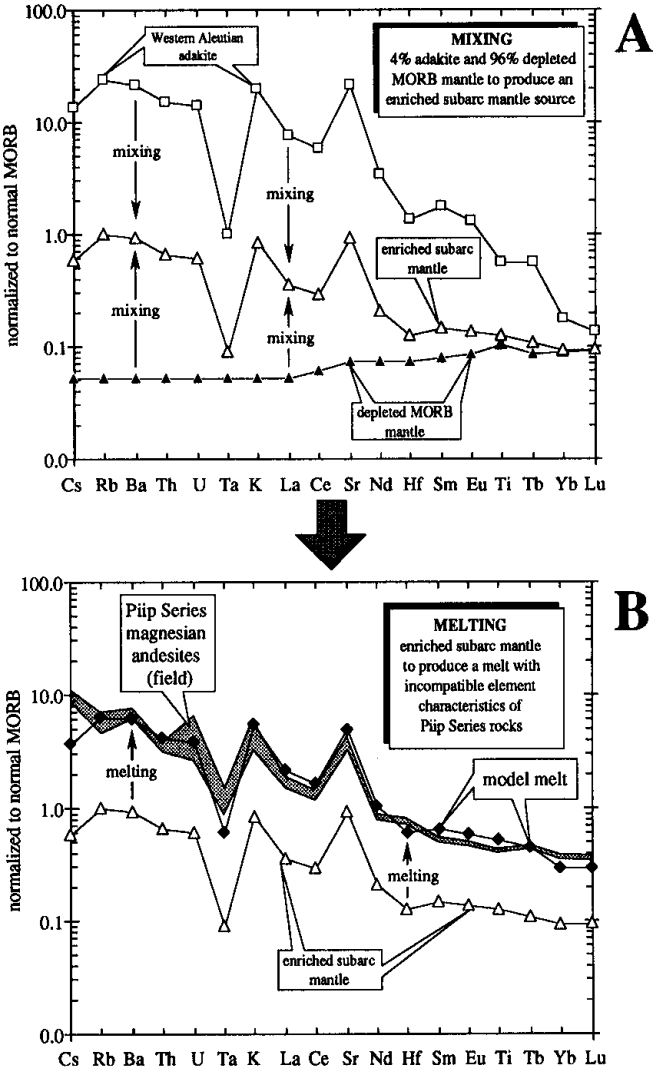

FIG. 15. Slab melt + mantle wedge model for the origin of the incompatible element characteristics of the Piip Series MA. In (A), mixture of 4% Western Aleutian adakite (same sample as in Fig. 14) and 96% depleted mantle (see below) produces an enriched subarc mantle source. In (B), batch melting (15%) of the enriched arc source produces an incompatible element pattern similar to that of the Western Aleutian MA [gray field in (B)]. Normalizing values are normal MORB of Hofmann (1988). Depleted mantle values are: Lu (0·054), Yb (0·347), Tb (0·077), Ti (1020), Eu (0·115), Sm (0·299), Hf (0·220), Nd (0·815), Sr (8·25), Ce (0·722), La (0·206), K (46·7), Ta (0·010), U (0·004), Th (0·010), Ba (0·734), Cs (0·0007). Depleted mantle REE, Ti, and Hf are from McKenzie & O'Nions (1991), Sr value assumes Sr/Nd = 10·13 (Hofmann, 1988), and all other elements give MORB ratios to La.

mineral was part of the residual mineralogy. Experiments of Rapp *et al.* (1991) have confirmed that vapor-absent melting of basalt at high pressures (32 kbar) and at 1050–1150°C will produce small volumes (<10%) of dacitic-to-rhyolitic melt that are saturated in garnet + clinopyroxene + rutile. With regard to rutile saturation and HFSE characteristics in arc magmas, these data confirm earlier findings of Green & Pearson (1986) and Ryerson & Watson (1987).

Melt–mantle interaction and magnesian andesites at Piip Volcano

Isotopic characteristics of the Western Aleutian rocks require that their source experienced a long-term history of chemical depletion, similar to that in MORB mantle (e.g., chondrite-normalized La/Yb $\ll 1$). The major element character of the Piip Series MA suggests that their source was a relatively fertile peridotite. The term 'fertile' is used here to indicate a lherzolitic source with mineralogic and major element characteristics similar to that which produced MORB (e.g., pyrolite).

The major element characteristics and mafic phenocryst compositions of the Piip Series MA suggest that they are near-primary melts of the Western Aleutian subarc mantle. It is well known that andesitic melts may form by peridotite melting under hydrous and low-pressure conditions (H_2O saturated or undersaturated; Green, 1976; Tatsumi, 1982), but increasingly it appears that primitive andesites and basaltic andesites may also form through the low-pressure reaction of basaltic melts and peridotite, even under anhydrous conditions (Fisk, 1986; Kelemen, 1986, 1990). This is because basalts saturated in olivine, two pyroxenes, and chromian spinel at high pressure become increasingly undersaturated in pyroxene as they rise to lower pressures. If such basalts pool within the warm upper mantle, they will undergo a mantle assimilation and fractional crystallization process (mantle-AFC) that will produce primitive silica-oversaturated melts and refractory peridotites (Kelemen, 1990).

Low CaO/Al_2O_3 and CaO/Na_2O, and high Na_2O and Al_2O_3 contents, suggest that the Piip Series MA formed by relatively small percentage melting of a fertile mantle source. In general, CaO/Al_2O_3 and CaO/Na_2O in primitive magmas are lowest at low percentage melting, but increase as clinopyroxene is melted from the residuum (Jaques & Green, 1980; Klein & Langmuir, 1987). If Na_2O is perfectly incompatible during peridotite melting, Piip Series MA would require a maximum of 10–11% batch equilibrium melting of MORB pyrolite ($Na_2O = 0{\cdot}39$; Falloon & Green, 1987). This estimate is similar to that for ocean ridge basalts produced at slow spreading centers by low percentage melting ($< 9\%$ melting at the Mid-Cayman Rise; Klein & Langmuir, 1987).

Chromian spinel compositions (Fig. 6) may provide further information on the source composition and/or the melting processes that produced the Western Aleutian lavas (e.g., Dick & Bullen, 1984). Chromian spinel inclusions in the MA are relatively Cr rich [$100Cr/(Cr + Al) \sim 60$] compared with Komandor Series basalts [$100Cr/(Cr + Al) \sim 40$; Fig. 6], but this implies a more advanced degree of melting for the MA, and/or a more refractory source than appears likely from the major elements (e.g., lower Ca/Al_2O_3 and higher Na_2O in the MA). Alternatively, high-Cr spinel inclusions in the MA might simply reflect the dependence of Cr partitioning on the SiO_2 content of the host melt (see fig. 8 of Dick & Bullen, 1984). If this is the case, the chromian spinel inclusions indicate that the peridotite source for both the Piip and Komandor Series lavas was a relatively fertile lherzolite similar to that which produces MORB.

Experimental data on MA confirm that low percentage melting of a relatively fertile source is a reasonable interpretation for the Piip MA data. Tatsumi (1982) interpreted the olivine–augite MA of the Japanese Setouchi Belt as small percentage melts in equilibrium with a lherzolitic residuum at 10 kbar and 1070°C, under water-undersaturated conditions ($\sim 7\%$ H_2O in the melt). On average, the Setouchi MA are slightly more primitive than the Piip Series MA (e.g., higher Cr and Ni), but they have all of the essential characteristics that distinguish the Piip Series MA from primitive basalts of the Central and Eastern Aleutians (see Fig. 16 and column 10 in Table 5).

A low-pressure origin is certainly consistent with the location of Piip Volcano on thin crust

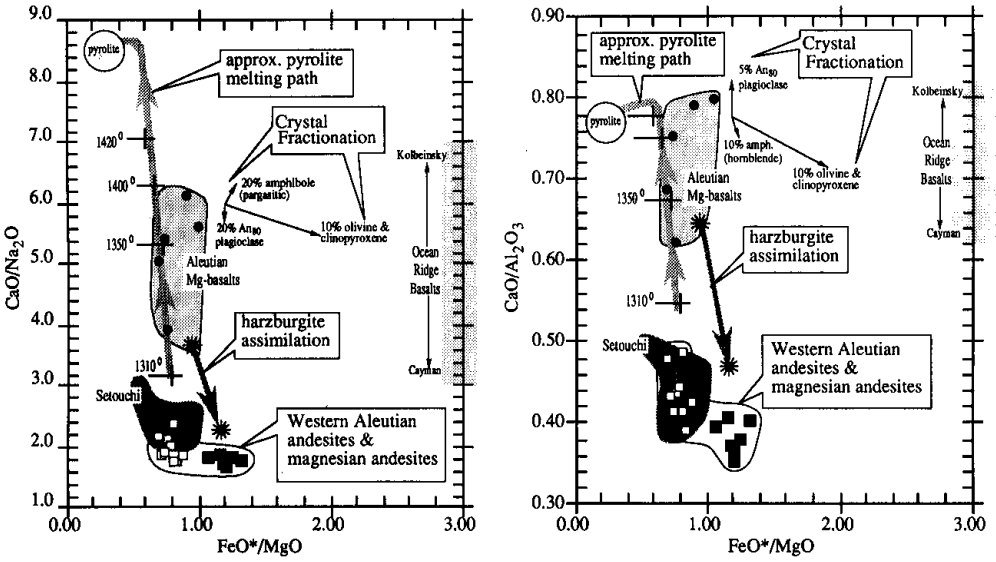

FIG. 16. CaO/Al_2O_3 and CaO/Na_2O vs. FeO*/MgO for Piip MA and Komandor Series andesites compared with primitive Aleutian Mg-basalts (Kay & Kay, in press), and Setouchi olivine–augite MA (Tatsumi & Ishizaka, 1982). Approximate melting paths for anhydrous peridotite (pyrolite) are from Falloon & Green (1987). Harzburgite assimilation trend is from SILMIN calculations in Kelemen (1990) with starting composition Aleutian Mg-basalt [MK15 in Gust & Perfit (1987); Kay & Kay (in press)] under conditions of decreasing temperature at 3 kbar. It should be noted that the steep trend produced by harzburgite assimilation in these diagrams cannot be reproduced by reasonable crystal fractionation processes. A similar trend is produced by SILMIN calculations of lherzolite assimilation (Kelemen, 1990). Range of CaO/Al_2O_3 and CaO/Na_2O ratios in ocean ridge basalts are from Klein & Langmuir (1987) (see columns 2 and 3 in Table 5).

(see Fig. 17 below). It is an important point, however, that MA also appear to have been parental melts in the Komandorsky and Near Islands, where the crust is not anomalously thin (see Yogodzinski *et al.*, 1993), and, more importantly, that primitive andesites and basaltic andesites are relatively common in the Cascades and in Mexico, where the arc crust is thick (e.g., Luhr & Carmichael, 1985; Hughes & Taylor, 1986; Hughes, 1990; Lange & Carmichael, 1990; Lopez & Cameron, 1992).

We conclude that, in general, primitive andesites like those at Piip Volcano are not produced by a simple, one-stage process of low-pressure hydrous melting of peridotite. In this regard, melt–peridotite interaction or mantle-AFC (i.e., Kelemen, 1986) is of interest, because it can produce the appearance of low percentage melting (as well as refractory chromite; Kelemen, 1990; Dick & Kelemen, 1991), but it may operate in arcs with widely variable crustal thickness (e.g., Western Aleutians, Japan, Cascades, and Mexico). The unifying feature of all arcs that produce MA and related rocks will be the tendency for melts of the mantle wedge to pool below the arc crust, where they will react with the ambient peridotite. This tendency may be promoted by compressive stresses in the arc crust and/or by thick crust.

In general, it appears that mantle-AFC reactions are capable of producing the essential characteristics that distinguish Piip Series MA from primitive basalts; these are high SiO_2 (54–58%) with low FeO*/MgO (<1), CaO/Al_2O_3 (<0·6), and CaO/Na_2O (<2·5). Kelemen (1990) showed that olivine will commonly dominate the crystallizing assemblage in mantle-AFC reactions, and that orthopyroxene will commonly dominate the assimilant. If, during the reaction, the mass assimilated equals the mass crystallized ($M_a/M_c = 1 =$ constant

TABLE 5

Natural and calculated compositions related to peridotite melting

	Ocean ridge basalts			*Aleutian Mg-basalts*				*Model*	*Primitive and other andesites and basaltic andesites*					
	1	2	3	4	5	6	7	8	9	10	11	12	13	14
SiO_2	48·20	50·04	51·30	48·97	48·46	50·28	51·20	55·11	56·64	58·42	55·85	57·7	55·81	52·10
Al_2O_3	16·30	14·98	16·25	16·25	15·14	16·10	15·69	17·61	16·95	15·90	19·48	17·4	17·52	16·44
FeO*	8·92	9·36	8·69	8·78	9·03	8·74	9·21	6·32	5·14	5·56	5·97	6·6	6·10	7·45
MgO	10·70	8·82	7·46	9·62	11·83	11·19	9·64	5·34	5·74	6·05	4·37	4·9	5·98	9·29
CaO	12·00	12·70	10·34	12·86	11·37	9·99	10·12	8·30	7·18	6·59	7·60	6·9	7·02	8·46
Na_2O	1·95	1·82	3·44	2·11	2·12	2·57	2·77	3·66	3·58	2·98	3·64	4·2	4·16	3·47
Sc (ppm)		45·		49·4	44·5	40·3			17·2	20·4	18·	20·5	16·3	28
FeO*/MgO	0·83	1·06	1·17	0·91	0·76	0·78	0·96	1·18	0·90	0·92	1·37	1·35	1·02	0·80
CaO/Al_2O_3	0·74	0·85	0·64	0·79	0·75	0·62	0·65	0·47	0·42	0·41	0·39	0·40	0·40	0·52
CaO/Na_2O	6·15	6·98	3·00	6·10	5·36	3·89	3·65	2·27	2·01	2·21	2·01	1·64	1·69	2·44

1. Primitive MORB glass ALV527-1-1 (Bender *et al.*, 1978).
2. North Atlantic MORB, Kolbeinsey Ridge (Sun *et al.*, 1979); example of ocean ridge high percent melt (Klein & Langmuir, 1987).
3. Average Mid-Cayman Rise basalt (Thompson *et al.*, 1980); example of ocean ridge low percent melt (Klein & Langmuir, 1987).
4. Primitive Aleutian basalt, Okmok Volcano, Umnak Island (Kay & Kay, in press).
5. Primitive Aleutian basalt, Adagdak Volcano, Adak Island (Kay & Kay, in press).
6. Primitive Aleutian basalt, Kanaga Island (Kay & Kay, in press).
7. Primitive Aleutian basalt, Makushin Volcano, Unimak Island (Gust & Perfit, 1987).
8. Model composition from primitive Aleutian basalt MK15 (No. 7 above) after harzburgite assimilation (table 3 of Kelemen, 1990).
9. Western Aleutian Piip Series magnesian andesite 2316/4 from Table 1.
10. Japan Setouchi Belt augite–olivine magnesian andesite SD-264 (Tatsumi & Ishizaka, 1982).
11. Central Oregon Cascades, North Sister-type basaltic andesite TS622 (Hughes, 1990).
12. Central Oregon Cascades, Mt. Washington-type basaltic andesite TS-631 (Hughes & Taylor, 1986).
13. Western Mexico basaltic andesite MAS 19 (Lange & Carmichael, 1990).
14. Michoacan, Mexico, Jorullo Volcano early stage basaltic andesite JOR44 (Luhr & Carmichael, 1985).

magma mass), the assimilation of orthopyroxene and crystallization of olivine may lower CaO/Al_2O_3 of the melt, but, in general, the crystallization of some clinopyroxene (at constant magma mass) would be required to lower CaO/Na_2O in the melt. Published thermodynamic models of mantle AFC processes [SILMIN calculations in table 3 of Kelemen (1990)] show that low-pressure reaction between a primitive Aleutian Mg-basalt and harzburgite, at decreasing temperature and magma mass ($M_a/M_c < 1$), will produce all of the essential major element characteristics that distinguish the Piip MA from primitive Mg-basalts of the Central and Eastern Aleutian arc (columns 7 and 8 in Table 5, and Fig. 16). Modeled basalt–lherzolite reactions under the same conditions produce the same trend (table 3, columns 2 and 3, of Kelemen, 1990). We believe that these results are general, and that they may account for the consistent occurrence of low CaO/Al_2O_3 and CaO/Na_2O ratios, and low Sc concentrations, in primitive basaltic and magnesian andesites from a variety of arcs (see comparison in Table 5). This result implies that refractory peridotites observed in certain alpine-type peridotites (e.g., Kelemen & Ghiorso, 1986), may in some way be complementary to a specific class of relatively common arc volcanic rocks. In Table 5 (columns 9–14) we have compiled examples of andesites which are broadly akin to the Piip MA and may also be the product of low-pressure melt–mantle interaction.

A summary of our model for the genesis of the Piip Series is presented in Fig. 17. As a

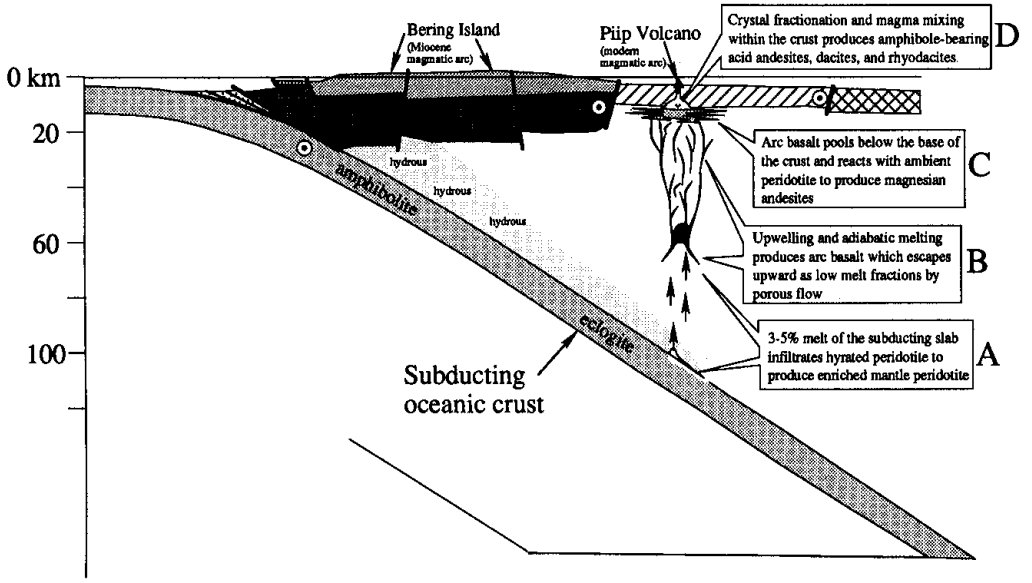

FIG. 17. Diagram of tectonics (no vertical exaggeration) of the Western Aleutian subduction zone with model for arc magma formation. Location of subducting slab was estimated from Boyd & Creager (1991). It should be recalled that, in the Western Aleutians, most of the motion is into and out of the plane of the page (noted by circled dot adjacent to known structures). In (A), small percentage melts formed at 1050–1150°C are dacitic to rhyolitic, and are saturated in garnet, clinopyroxene, and rutile (e.g., Rapp *et al.* 1991). The silicic slab melt infiltrates and reacts with hydrous peridotite above the slab. In (B), a broad zone upwelling causes adiabatic melting to produce high-Mg arc basalts that drain upward by porous flow at relatively low melt fractions. In (C), the arc basalt is trapped below the crust–mantle boundary, as a result of compressive stresses in the arc. At this pressure, the arc basalt is undersaturated in pyroxene, so it reacts with the ambient peridotite to produce a smaller volume of MA at lower temperature. In (D), MA fractionate to produce amphibole-bearing acid andesites, dacites, and rhyodacites of Piip Volcano.

general model for arc magma formation, this model most closely resembles those first proposed by Ringwood (1974). The model begins with melting of the subducting slab to produce a small volume of rhyolitic magma that infiltrates the mantle wedge (Fig. 17A). Reaction between the slab melt and the hot mantle wedge produces a chemically enriched, arc peridotite source. Upwelling of this enriched source creates a broad zone of adiabatic melting to produce arc basalt which escapes upward by porous flow at relatively low melt fractions (Fig. 17B). The arc basalt pools within the uppermost mantle, as a result of compressional stresses within the crust (Fig. 17C). In the low-pressure regime of the uppermost mantle, the basalt is undersaturated in pyroxene, so that if it remains trapped for a sufficient duration, mantle-AFC reactions will produce increasingly silica-oversaturated melts. In the extreme case, such as at Piip Volcano, primitive arc basalts at high temperatures (>9% MgO, ~1200°C) are transformed into a smaller volume of MA at lower temperatures (6–7% MgO, ~1050–1150°C). Eventually, the MA migrate into the lower and middle crust, where they fractionate at low temperatures (<1000°C, >7 km depth) to produce small volumes of hornblende-bearing rhyodacites, dacites, and acid andesites which make up most of the Piip Volcano edifice (Fig. 17D, fractionation model in Fig. 18; see below and Romick *et al.*, in press).

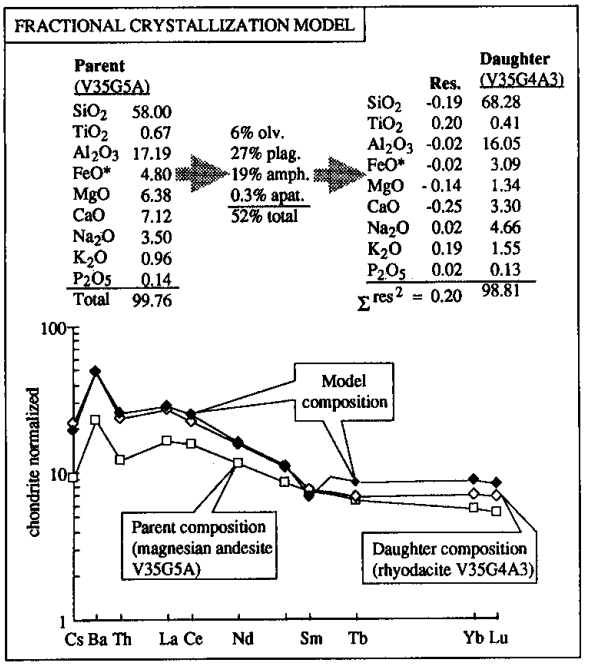

FIG. 18. Least-squares major element model beginning with MA (parent) produces rhyodacite (daughter) by 52% closed-system fractionation of plagioclase- and amphibole-dominated mineral assemblage. Trace element model is based on fractionating assemblage determined by major elements. Modeling parameters are given in Table 6.

It is likely that a continuum of crystallization and assimilation processes takes place immediately below and within the arc crust, but the physical configuration of the melt and country rock, and the ambient thermal conditions probably allow significant assimilation of mantle peridotite, but only minor assimilation of arc crust (Kelemen, 1990). In general, mantle-AFC reactions are energetically favored in the warm upper mantle and will be further enhanced if the melt resides along grain boundaries of the peridotite country rock. In crustal-

level magma chambers, temperatures are lower so that assimilation will be energetically more difficult. This will be especially true if in crustal magma chambers the melt resides largely within its own crystal mush and is physically armored from the crustal country rock.

With regard to the origin of calc-alkaline magmas, this model differs from that of Kay *et al.* (1982) and Kay & Kay (1985) only in that mantle AFC is required to produce the strongly calc-alkaline characteristics of the Western Aleutian andesites and MA (e.g., Fig. 16). Implicit in this model is the idea that magmatic style (calc-alkaline vs. tholeiitic) is dependent to a large degree on the tectonic regime within the arc (Kay *et al.*, 1982; Kay & Kay, 1985; see also the discussion below). Many calc-alkaline volcanoes in the Aleutians are located in areas where magma ascent from the mantle may be inhibited by compressive stresses in the arc crust (Kay *et al.*, 1982; Geist *et al.*, 1988; Romick *et al.*, 1992; Singer & Myers, 1992). If primitive basaltic melts are trapped in the uppermost mantle, where they may react with residual peridotite, they will become more calc-alkaline (i.e., higher SiO_2 relative to FeO*/MgO) than in areas where magma ascent through the crust is uninhibited (see also Myers *et al.* (1985)). If Piip Volcano provides an extreme case of calc-alkaline magmatism in the Aleutians, then the presence of primitive andesites (not primitive basalts) is expected from a mantle assimilation model for calc-alkaline magmatism (Kelemen, 1990).

Origin of the strongly calc-alkaline series

Broad similarities between Piip Volcano and calc-alkaline volcanoes of the Central and Eastern Aleutians suggest that processes which produce calc-alkaline magmatism are similar throughout the arc. The presence of amphibole phenocrysts, phenocryst-rich textures, and abundant evidence for magma mixing such as bimodal phenocryst populations and phenocryst–whole-rock disequilibrium, are all features of evolved members of the Piip Series (>59% SiO_2) which are also common in calc-alkaline rocks of the Central and Eastern Aleutians. These characteristics imply that crystallization of calc-alkaline series magmas occurs at relatively low temperatures in broadly open magma systems deep within the arc crust (Kay *et al.*, 1982; Kay & Kay, 1985; Romick *et al.*, 1992).

Regional isotopic differences aside, the only fundamental distinction between calc-alkaline magmatism at Piip Volcano and in the Central Aleutians is the nature of the parental magma. The volumetric dominance of high-Al basalt, formed by crystal fractionation of Mg-basalt, suggests that Mg-basalts are the important parental magmas at calc-alkaline volcanoes in the central and eastern arc (Kay *et al.*, 1982; Conrad & Kay, 1984; Kay & Kay, 1985, in press; Miller *et al.*, 1992). The strongly calc-alkaline trend at Piip Volcano (FeO*/MgO = 1·2 at 65% SiO_2) was produced by the removal of an amphibole-bearing mineral assemblage from a parental MA with 57% SiO_2 and FeO*/MgO ~0·8 (Fig. 4). Least squares modeling indicates that 52% closed-system fractionation of plagioclase (27%), amphibole (19%), olivine (6%) and apatite (0·3%) from a Piip Series MA will closely reproduce the major element characteristics of the Piip Series rhyodacites [Fig. 18; see also the MA to dacite model of Romick *et al.* (in press)]. This type of model reproduces the LILE, LREE, and the overall shape of the REE pattern well (Fig. 18), but the calculated HREE concentrations are higher than observed, suggesting some inaccuracy in distribution coefficients for these elements in amphibole and/or apatite (modeling parameters in Table 6).

Amphibole fractionation has long been recognized as an important aspect of the calc-alkaline igneous rock series (see recent review by Romick *et al.*, 1992). Kay *et al.* (1982), Conrad & Kay (1984), Kay & Kay (1985), and Romick *et al.* (1992) have all emphasized early fractionation of amphibole to produce not only silica enrichment at low FeO*/MgO, but also a characteristic increase in La/Yb over a relatively narrow range of La concentrations

TABLE 6

Modeling parameters

	Mineral compositions				*Mineral/liquid distribution coefficient*†*				
	1 *amph*	2 *plag*	3 *olv*	4 *apat*		5 *amph*	6 *plag*	7 *olv*	8 *apat*
SiO_2	47·57	53·28	39·10	—	La	0·54	0·274	0·007	42·07
TiO_2	1·46	—	—	—	Ce	0·84	0·279	0·007	52·50
Al_2O_3	7·58	30·36	—	—	Nd	1·34	0·290	0·007	81·80
FeO*	11·74	0·48	15·28	0·22	Sm	1·80	0·144	0·007	89·80
MgO	15·68	0·17	44·26	0·53	Eu	1·56	2·490	0·007	50·20
CaO	10·78	13·26	0·13	54·84	Tb	2·02	0·099	0·009	73·86
Na_2O	1·59	3·62	—	0·20	Yb	1·64	0·056	0·014	37·00
K_2O	0·17	0·01	—	—	Lu	1·56	0·054	0·016	30·00
P_2O_5	—	—	—	35·01					

1. Hornblende from Piip Volcano dacite.
2. Plagioclase, An_{67}.
3. Olivine, Fo_{84} from Piip magnesian andesite.
4. Apatite (Deer *et al.*, 1966).
5. Fujimaki *et al.* (1984).
6. Nagasawa & Schnetzler (1971).
7. Arth (1976).
8. Nagasawa (1970).

*Some values estimated by interpolation or extrapolation.
†Assumed to be zero for Cs, Ba, and Th.

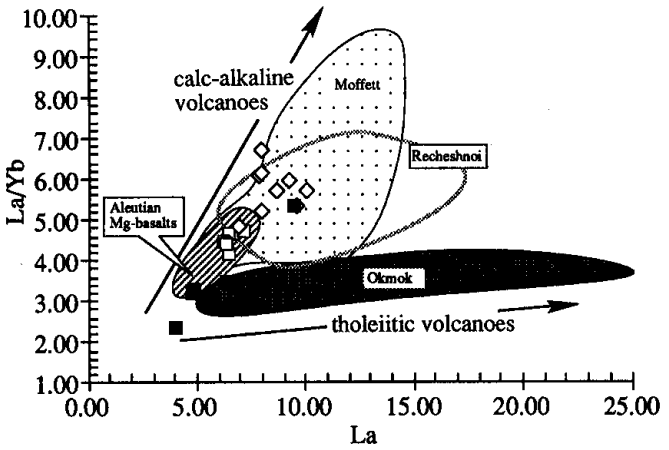

FIG. 19. Contrasting variation in REE in tholeiitic and calc-alkaline systems in the Aleutian arc. Western Aleutian data (Table 1, symbols as in Fig. 4) show significant increase in La/Yb over a narrow range of La concentration, similar to that of Central and Eastern Aleutian calc-alkaline volcanoes (Moffett—Kay & Kay, in press; Recheshnoi—Miller *et al.*, 1992). At Piip Volcano, increasing La/Yb results from amphibole fractionation. In Komandor Series rocks, La/Yb variation reflects source composition (see text and Fig. 8). The significant La/Yb variation even among primitive Aleutian Mg-basalts should be noted (Kay & Kay, in press). Tholeiitic trend (Okmok—Miller *et al.*, 1992) reflects low-pressure fractionation of anhydrous mineral assemblage.

[Fig. 19; see also fig. 5 of Miller *et al.* (1992)]. A key feature of the melt–peridotite reaction process is that as hot primitive melts cool, they are buffered at low FeO*/MgO by reaction with peridotite. Under these conditions, fractionation of amphibole ± Fe–Ti oxides (which occurs only at relatively low temperatures) can produce Si enrichment at low FeO*/MgO (i.e., the calc-alkaline trend). Without the assimilation of peridotite, fractionation of olivine will generally force the melt to evolved (high FeO*/MgO) compositions. Amphibole fractionation is thus likely to be promoted in an igneous rocks series that begins in the uppermost mantle with AFC reactions (see also Kelemen & Ghiorso, 1986).

Mantle–AFC reactions may play some role in the formation of calc-alkaline volcanic rocks in the Central and Eastern Aleutians, but they probably have not gone so far as to produce mantle-derived andesites such as those at Piip Volcano. The predominance of parental MA at Piip Volcano and in the Western Aleutian Komandorsky and Near Islands since Middle Miocene time (Yogodzinski *et al.*, 1993), suggests that transpressional tectonic conditions prevent the transport of basaltic melts through the arc crust, and promote the mantle-AFC reactions which produce MA and the strongly calc-alkaline Western Aleutian trend (see fig. 15 of Yogodzinski *et al.*, 1993).

DISCUSSION AND IMPLICATIONS

Western Aleutian tectonics and the mantle wedge

The predominantly MORB-like isotopic characteristics of the Western Aleutian rocks readily distinguish them from those in other parts of the Aleutians and from other arcs. Ultimately, this isotopic signature may reflect important aspects of Western Aleutian tectonics, including the highly oblique convergence angle, and the relatively young age of the Western Aleutian subduction system.

Oblique convergence in the Western Aleutians results in low subduction rates, and low recycling rates compared with the central and eastern arc. If the subduction zone effectively filters and regulates the geochemical character of subducted material (Kay, 1980; Saunders *et al.*, 1987; Morris *et al.*, 1990), then the long, slow subduction path beneath the Western Aleutian forearc may have mechanically and chemically stripped the loosely bound components from the surface of the subducting lithosphere. In the Western Aleutians, the sediment column on the subducting plate is relatively thin, so that highly oblique convergence may result in particularly low recycling rates for those elements that are concentrated in sediment (e.g., Cs).

It is an important additional point that subduction beneath the far Western Aleutians was probably established only 10–20 Ma ago (Cooper *et al.*, 1992; Yogodzinski *et al.*, 1993), and that this is consistent with the subducting slab geometry beneath the Western Aleutian region today (Creager & Boyd, 1991). It may be that low subduction and recycling rates over a relatively short lifetime have left the Western Aleutian sub-arc mantle relatively unaltered compared with that of the Central and Eastern Aleutians, where subduction has occurred for ~50 my (Scholl *et al.*, 1987; Vallier *et al.*, in press). This is consistent with findings in the Central Aleutians, where the early magmatic rocks of the arc are geochemically less enriched (lower Ba/La and Th/La ratios) than volcanic rocks of the modern arc (Kay & Kay, in press). This kind of secular variation may imply that the magma source depends not only on the composition of the mantle wedge and the subducting lithosphere, but also on the integrated effects of recycling over the lifetime of the arc. Some elements may have long residence times in the mantle wedge, and will continue to appear even in post-subduction lavas (e.g., K and Sr), whereas others may be effectively stripped from the system at shallow levels (e.g., boron; Morris *et al.*, 1990). Romick *et al.* (in press) interpreted the subduction component in Piip

dacites as one that had been stored in the back-arc mantle from a previous subduction episode. With the recognition of an aseismic slab beneath the Western Aleutians (Boyd & Creager, 1991), the stored component interpretation becomes unnecessary. None the less, secular change in mantle wedge chemistry through the recycling and storage of geochemical components remains an important concept in the interpretation of arc magma geochemistry and the evolution of subduction systems.

It appears then that in the unique Western Aleutian tectonic geometry, Piip Volcano has sampled a MORB-like mantle wedge that has remained largely uncontaminated by recycling of components of continental origin. This is an important conclusion, because in the well-studied Central and Eastern Aleutians, mixing and melting processes in the subduction environment are complex and complete to the extent that the unaltered composition of the mantle wedge cannot be unambiguously deduced from the chemistry of the arc volcanic rocks (e.g., Morris & Hart, 1983; Perfit & Kay, 1986). By extrapolation, we suggest that with respect to its incompatible and isotopic characteristics, the Central and Eastern Aleutian mantle wedge is also similar to the depleted MORB mantle (see also Yogodzinski *et al.*, 1993).

HFSE and the subduction component: slab melts, slab-derived fluids, and/or a highly depleted source?

Low HFSE concentrations in arc volcanic rocks compared with MORB have long been thought to originate in some way in a previously melted and therefore highly depleted arc peridotite source (e.g., Green, 1976). Kelemen *et al.* (1990), for example, have shown that basaltic melts that react with a large mass of refractory peridotite will become progressively depleted in HFSE and heavy REE, whereas the light REE concentrations remain largely unchanged (e.g., fig. 2 of Kelemen *et al.*, 1990). To produce the observed fractionation between largely incompatible elements (e.g., La and Ta), this process requires very large rock–melt reaction ratios (100–200). We believe that such high reaction ratios may be unrealistic, and we note that melt–rock ratios of this magnitude are probably not required to produce significant fractionation among the major elements (e.g., decreasing CaO/Al_2O_3 in Fig. 16). More importantly, however, the melt–peridotite interaction process (as it has been applied to HFSE in arc magmas) is one of selective depletion, and is therefore qualitatively unlike the selective enrichment process which apparently produces the chemical signature of many arc volcanic rocks. Figure 8B, for example, shows the development of the arc signature in a series of andesites as a progressive increase in La and Th at nearly constant Ta and Yb. This kind of variation is not consistent with the process proposed by Kelemen *et al.* (1990), but it is consistent with enrichment by a slab melting model shown in Fig. 15.

Salters & Shimizu (1988) have suggested that HFSE-depleted peridotite is a ubiquitous (world-wide) feature of the upper mantle, and that fluid-induced melting of this material at convergent margins produced HFSE-depleted arc volcanic rocks. If HFSE-depleted mantle peridotite is widespread in the upper mantle (a point that is certainly contested, e.g., McDonough, 1990), then it is difficult to see why this source would be commonly sampled at convergent margins and never at ocean ridges. We assume that the mantle source beneath arcs is largely asthenospheric; this is required because arcs commonly produce basalts for tens of millions of years at a single location without any apparent source depletion (e.g., Hawkins *et al.*, 1984; Gill, 1987; Kay & Kay, in press). Indeed, the most refractory arc magmas (boninites) are characteristic of the early (not the late) stages of arc evolution (Hawkins *et al.*, 1984). If the major element source for arc basalts is the mantle wedge, then replenishment of the mantle wedge by asthenospheric flow is required over the lifetime of an

arc. If ubiquitous upper-mantle asthenosphere beneath the oceans is that which produces MORB, then it is likely that this is the material that is channeled into the mantle wedge, where it is selectively enriched by slab-related processes.

In the slab melt + mantle wedge model (Fig. 15), the HFSE-depleted and LILE-enriched characteristics of arc volcanic rocks are inherited from silicic, small percentage melts of the subducting slab which are saturated in garnet, clinopyroxene, and rutile (or some other Ti-rich mineral). These characteristics for slab melts are consistent with experimental data (Green & Pearson, 1986; Ryerson & Watson, 1987; Rapp *et al.*, 1991), and with the incompatible element character of Aleutian adakites (Figs. 14 and 17). McCulloch & Gamble (1991) have argued that residual rutile does not play a role in subduction systems, because arc lavas do not show dramatic fractionation among HFSE (e.g., very low Ti/Zr). We note, however, that the addition of a rutile-saturated slab melt ($\sim$0·90% TiO_2; table 2 of Rapp *et al.*, 1991) to a MORB-like mantle wedge will not produce dramatic fractionation among the HFSE, but will produce a peridotite source with substantially depressed HFSE/REE ratios (especially Ta/La; Fig. 15).

Arculus & Powell (1986) and Ringwood (1990) have noted that HFSE retained in high-Ti minerals within the subducting slab would eventually be released at deeper levels where they could contribute to the formation of intraplate magmas which commonly are HFSE enriched. Reagan & Gill (1989) concluded that Ti-rich minerals were stable not within the subducting slab, but in a zone of hydrous and oxidized peridotite immediately above the subducting slab. Therefore, the Ti-rich minerals might break down under the influence of reducing, CH_4-bearing melts from the deep asthenosphere, and could contribute to the formation of high-Nb basalts within the arc (Reagan & Gill, 1989). The occurrence of high Ti–Ta–Nb volcanic rocks in unusual tectonic positions in some arcs (Verma & Nelson, 1989), and/or in some back-arc areas (Nakamura *et al.*, 1989; Coira & Kay, 1993) also suggests that Ti-rich minerals which are stable under the main volcanic front eventually break down as a result of changing thermal or f_{O_2} conditions (e.g., Ringwood, 1990). On the basis of the experimental data and the characteristics of Aleutian adakites, we conclude that residual Ti-rich phases are stabilized within the subducting slab, but we agree that under certain circumstances, especially increasing temperature and decreasing f_{O_2}, they may break down to form HFSE-enriched melts within the arc or near-arc setting.

The HFSE-depleted and LILE-enriched character of arc volcanic rocks more commonly are attributed to fluid-dominated mass transport from the slab, into the mantle wedge (e.g., Tatsumi *et al.*, 1986; Stern *et al.*, 1991). Although it is clear that water is an important aspect of the petrology and geochemistry of arc magmas, it is not clear that mass transport by hydrous fluids is an adequate explanation for many characteristics of arc volcanic rocks. Supporters of the fluid metasomatism theory may argue that in addition to high ratios of alkali and alkaline-earth elements to REE (e.g., high Sr/Nd), slab-derived fluids (not melts) are required to explain the characteristically low HFSE to REE ratios of arc magmas. It should be noted, however, that Cs, K, and Sr spikes occur in Western Aleutian basalts and basaltic andesites which are not low in Ta or Ti compared with the REE (Fig. 10). Potassium enrichment in these rocks is equivalent to that in basalts of the central and eastern arc (e.g., K/La in Fig. 9), and apparently was produced without significantly affecting the HFSE/REE ratios of the MORB-like source (Fig. 10). This observation argues against general models in which alkali element enrichments in arc magmas are coupled to relative HFSE depletions by fluid-dominated processes of selective enrichment (e.g., Tatsumi *et al.*, 1986).

Stern *et al.* (1991) presented a more complex fluid metasomatism model using the relative fluid/serpentinite distribution coefficients inferred from Tatsumi *et al.* (1986). In this model, slab-derived fluids chemically infiltrate and react chromatigraphically with mantle solids to

produce the trace element and isotopic characteristics of the subduction component in Mariana boninites. The experiments of Watson & Brenan (1987) indicate, however, that the wetting characteristics of H_2O–CO_2 fluids in the mantle will generally not produce the interconnected fluid network that is required for chromatographic processes to operate. Watson & Brenan (1987) concluded that even in the asthenospheric mantle, fluids will generally reside in isolated pores that will remain largely unconnected except during transient episodes of flow by hydrofracture.

Magmas, on the other hand, may form highly interconnected networks in the asthenospheric mantle, and may move efficiently by grain boundary infiltration, even at low melt fractions (McKenzie, 1984). Their greater mobility and greater potential for interaction with a large mass of solid mantle implies that melts are more likely than fluids to produce the surprisingly homogeneous subduction components observed in the Aleutians and in other arcs (Kay & Kay, 1988, in press; Morris *et al.*, 1990; Stern *et al.*, 1991). In particular, Kay & Kay (1988, in press) have observed systematic regional behavior of Ba, Th, and U in Central and Eastern Aleutian basalts and basaltic andesites, and have noted that these elements are strongly fractionated in marine sediments, hydrothermal fluids, and seawater. In this regard, we note the uniform behavior of Ba, Th, and U in the Western Aleutian rocks (compare with Cs, K, and Sr in Fig. 10), and the similarity of Ba/Th throughout the modern volcanic suite in the Aleutians (Fig. 9B). If the budgets for such geochemically diverse elements in arc magmas are dominated by the subduction component (e.g., Kay, 1980; Stern *et al.*, 1991), then observed regional similarities imply a mixing process that may be more efficiently accomplished by melts, which have high concentrations of these elements compared with high-pressure fluids.

Finally, the most direct measure of fluid control in subduction systems may be provided by highly soluble elements such as B and He. Although data for these elements are not available for Western Aleutian rocks, it is an important point that $^3He/^4He$ in arc rocks generally require negligible He input from the subducting plate, and that B concentrations are extemely low in rocks erupted behind the main magmatic front (Poreda & Craig, 1989; Morris *et al.*, 1990). These elements, which are efficiently transported by fluids, are apparently not recycled into the deeper parts of the subduction system (or into the deep mantle; Morris *et al.*, 1990) even though the subduction trace element signature persists well into the rear magmatic zone (e.g., high Ba/La in Bogoslof samples; Kay & Kay, in press). It may be that fluid transport dominates only at shallow levels where water and highly soluble elements are largely expelled from the system, and that more deeply subducted components, such as K, are transported from the slab to the mantle wedge principally by melts. In this regard, low H_2O/K_2O in arc basalts and MORB compared with those of metasomatic fluids, are taken as good evidence that fluid transport typically does not control the K_2O budget in the source of arc volcanic rocks (e.g., Michael, 1988; Eggler, 1989).

Crustal thickness, melt–mantle interaction, and calc-alkaline vs. tholeiitic magmatism in arcs

The model presented in Fig. 17 is similar to that proposed by Kay *et al.* (1982), Conrad & Kay (1984), and Kay & Kay (1985), in that the calc-alkaline and tholeiitic trends are developed at relatively shallow levels in the subduction system (Figs. 17C and D). The calc-alkaline trend is produced when high-Mg arc basalts are trapped in the uppermost mantle and lower crust by compressive stresses within the arc. Under these conditions, mantle-AFC reactions and crust-level fractionation at low temperatures near the crust–mantle boundary produce relatively small volumes of volcanic rock which commonly contain amphibole. Such

a system will typically produce a small volcano, but probably a large calc-alkaline pluton (small extrusive/intrusive ratio). In contrast, the tholeiitic trend dominates areas where arc crust is extended, and relatively large volumes of hot, primary arc basalt rise rapidly to mid-crustal or upper-crustal magma chambers where they fractionate anhydrous minerals at high temperatures and low pressures (Kay *et al.*, 1982; Kay & Kay, 1985; Singer & Myers, 1992). The tholeiitic system will generally produce a large volcano, but only a very small pluton. In sum, we regard the extrusive/intrusive ratios and broad major element differences between calc-alkaline and tholeiitic systems as prima facie evidence that the ease with which melts are transported into and through the crust exerts substantial influence over magma evolution, even within oceanic arcs where the crust is relatively thin.

The importance of crustal thickness in arc magma genesis has long been recognized (e.g. Green, 1982; Leeman, 1983). Most recently, Miller *et al.* (1992) developed the idea that primitive basalts of calc-alkaline systems are produced by smaller percentage melting than those in tholeiitic systems, and that this eventually produces the distinctive tholeiitic and calc-alkaline geochemical trends (e.g., Figs. 4 and 19), as well as the physical manifestations of tholeiitic and calc-alkaline magmatism (i.e., volcano size, mineral assemblage, etc.). Miller *et al.* (1992) also noted that on a global scale (data from Plank & Langmuir, 1988), arcs built on thick crust have a tendency to be more calc-alkaline (lower FeO*, higher SiO_2) compared with those built on thin crust. This is consistent with the Plank & Langmuir (1988) model, wherein thick arc crust and a short melting column within the mantle wedge produce basalts by smaller degrees of melting than in arcs where the crust is thin and the melting column is longer.

Piip Volcano is built on back-arc type crust of the Komandorsky Basin (7–15 km thick?), which is perhaps the thinnest crust anywhere, upon which an arc volcano is built (see compilation by Plank & Langmuir, 1988). According to the Plank & Langmuir (1988) model, this should result in a long melting column, to produce high-CaO, low-Na_2O and low-SiO_2 arc basalts by large percentage melting; however, the opposite occurs, as the important primary magmas at Piip Volcano are MA with low CaO, and high Na_2O and SiO_2. More mafic rocks in the Piip Volcano area also have these tendencies (Table 1). The location of Piip Volcano 100–130 km above the subducting slab (Boyd & Creager, 1991) is like that of arc volcanoes world-wide, so in this regard Piip is a typical arc volcano. It is an important point, however, that mantle wedge dynamics beneath the Western Aleutians may be unusual, because very little of the slab's motion is directed downward into the mantle (see Fig. 17). Melting within the mantle wedge beneath Piip Volcano may therefore be unlike that inferred by Plank & Langmuir (1988). We emphasize, however, that primitive andesites, and strongly calc-alkaline volcanism like that at Piip Volcano, are common in some areas where subduction is not highly oblique (e.g., Oregon Cascades and Western Mexico).

Plank & Langmuir (1988) recognized a systematic tendency toward high Na_2O and SiO_2, and low CaO in some arcs, in particular, in New Zealand and Mexico, but they attributed this to a crustal overprint rather than a primary mantle process. We note, first, that primitive andesites and basaltic andesites in Mexico (e.g., columns 13 and 14 in Table 5) usually contain Mg-rich mafic phenocrysts consistent with a mantle origin (Luhr & Carmichael, 1985; Lange & Carmichael, 1990), and, second, that SiO_2–Na_2O–CaO systematics of this kind are a logical consequence of mantle-AFC reactions like those that have produced MA at Piip Volcano. These characteristics are perhaps most striking in the Central Oregon Cascades, where basaltic andesites (e.g., columns 11 and 12 in Table 5) commonly have mafic phenocrysts that are more primitive (higher *mg*-number) than the associated basalts (Hughes & Taylor, 1986; Hughes, 1990).

According to Miller *et al.* (1992), the long melting column beneath Piip Volcano should

produce large percentage melting in the mantle wedge and, as a consequence, a strongly tholeiitic series. As noted above, Piip Volcano is the most strongly calc-alkaline volcano in the Aleutians. In our view, adjacent volcanoes of tholeiitic and calc-alkaline affinity like those studied by Miller *et al.* (1992), reflect local zones of tectonic compression and dilation which are produced by oblique subduction in the Central and Eastern Aleutian arc (Geist *et al.*, 1988). We agree that calc-alkaline volcanoes have some characteristics consistent with low percentage melting (Miller *et al.*, 1992), but note that mantle-AFC reactions will also produce these characteristics. In particular, low CaO/Al_2O_3 and CaO/Na_2O in the Piip MA are low percentage melting features (e.g., Klein & Langmuir, 1987), but may also be produced by mantle-AFC processes (Fig. 16).

By extending the fractionation–mixing–assimilation processes of Kay *et al.* (1982) into the uppermost mantle, where assimilation of mantle materials is likely (Fig. 17D), the whole spectrum of geochemical and physical distinctions between tholeiitic and calc-alkaline systems can be accounted for. In Fig. 20, the major element distinctions between Aleutian

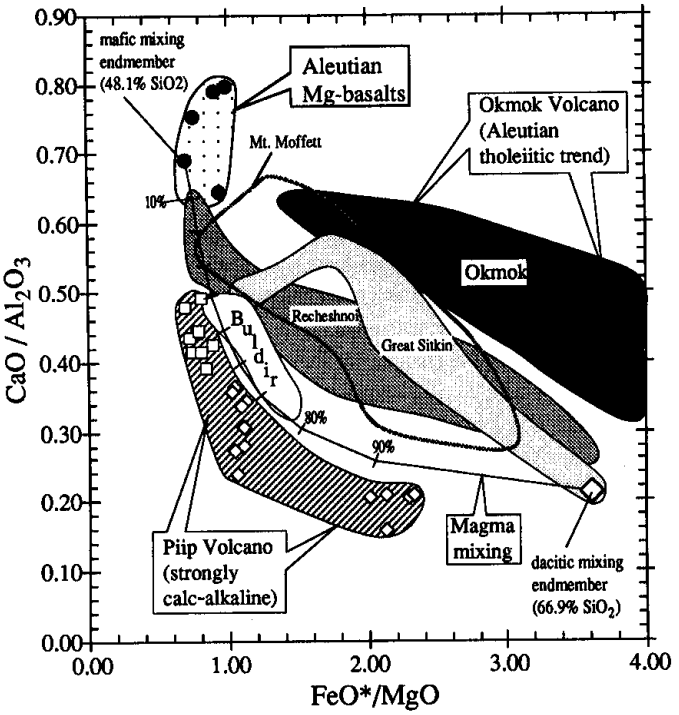

FIG. 20. Comparison of differentiation trends in Aleutian tholeiitic (Okmok), calc-alkaline (Great Sitkin, Moffett, and Recheshnoi), and strongly calc-alkaline (Piip and Buldir) Aleutian volcanoes. Mixing line is between Mg-basalt from Okmok Volcano (Eastern Aleutians) and dacite from Great Sitkin Volcano (Central Aleutians). Okmok and Recheshnoi data are from Miller *et al.* (1992); Great Sitkin, Mt. Moffett, and Buldir data are from Kay & Kay (1985, in press).

tholeiitic and calc-alkaline systems are illustrated by a plot of the CaO/Al_2O_3 vs. FeO*/MgO. High CaO/Al_2O_3 in the tholeiitic trend is interpeted to reflect a plagioclase-dominated (low-pressure) fractionation series, consistent with the development of large Eu anomalies in evolved tholeiitic lavas (Carr *et al.*, 1982; Kay *et al.*, 1982; Kay & Kay, in press). Lower CaO/Al_2O_3 in the calc-alkaline volcanoes (Moffett, Recheshnoi, and Buldir), reflects a higher-pressure fractionation series in which the role of plagioclase is diminished relative to

that of clinopyroxene and amphibole. At Piip Volcano, the primitive characteristics of the MA require that the fractionation series began with AFC reactions in the uppermost mantle (see above). From this, we conclude that the gap in primitive Aleutian rock compositions between Mg-basalts and Western Aleutian MA (e.g., $CaO/Al_2O_3 = 0{\cdot}5$–$0{\cdot}6$ in Fig. 20) is more likely to be filled by parental magmas at calc-alkaline than at tholeiitic centers. A small number of calc-alkaline andesites from Recheshnoi, Moffett, and Buldir volcanoes do fall in this compositional range, but they show substantial mineralogical and textural evidence for magma mixing, and cannot unambiguously be characterized as MA (see Kay & Kay, 1985, in press; Miller *et al.*, 1992). Indeed, the Buldir trend in Fig. 20 can be interpreted entirely as a mixing line between Mg-basalts and silicic melts (Kay *et al.*, 1982; Kay & Kay, 1985). On the basis of our results from Piip Volcano, we suggest, however, that parental melts at Buldir Volcano may have major-element characteristics that are broadly transitional between Aleutian Mg-basalts and Piip Series MA (e.g., $\sim 51\%$ SiO_2, $CaO/Al_2O_3 \sim 0{\cdot}54$, and $CaO/Na_2O \sim 3{\cdot}0$), and that these parental melts were produced when high-Mg basalts underwent mantle-AFC reactions similar to those that produce MA at Piip Volcano.

CONCLUSIONS

Fractionation of parental magnesian andesites (MA) at Piip Volcano in the strike-slip Western Aleutians has produced a more strongly calc-alkaline magma series (lower average FeO*/MgO) than any in the Central or Eastern Aleutian arc. Compositions of the Western Aleutian MA are consistent with formation by basalt–peridotite reaction in the uppermost mantle. The predominance of MA as parental magmas throughout the Western Aleutians since Middle Miocene time (Yogodzinski *et al.*, 1993), suggests that broadly transpressional tectonics within the western arc causes primitive basaltic melts of the mantle wedge to pool in the uppermost mantle where they interact with warm, ambient peridotite to produce highly silica-oversaturated lavas of mantle origin (MA). Very thin crust beneath Piip Volcano has not produced any of the proposed consequences of a long melting column in the mantle wedge (e.g., high percentage melting and tholeiitic volcanism—Plank & Langmuir, 1988; Miller *et al.*, 1992).

Isotopic constraints require that volcanic rocks of the Piip Volcano area were formed by a mixture of two broadly MORB-like sources—(1) the subducting slab, and (2) the overlying mantle wedge. Simple mixing models require that the LILE in the Western Aleutian rocks originated overwhelmingly in the basalt–gabbro portion of the subducting slab, and that they were added to the mantle wedge source in relative abundances similar to those in normal MORB. This is most easily accomplished by small percentage melting of the subducting slab. Mixtures of Western Aleutian adakite (hypothetical slab melts) and depleted MORB mantle can produce an enriched peridotite source with isotopic and inter-element ratios (including HFSE depletions) consistent with the source of Western Aleutian lavas.

These results provide an improved basis for understanding the geochemistry of volcanic rocks from normal arc settings. Strong HFSE depletions in Aleutian adakite are taken as good evidence that slab melts, saturated in clinopyroxene + garnet + rutile, infiltrate the mantle wedge and are responsible for much of the HFSE-depleted and LILE-enriched incompatible element signature of arc volcanic rocks. It is an important point, however, that by mass-balance, a slab melt of this kind will make only a minor contribution (mostly in K_2O) to the major element budget of arc magmas. In this way, the slab melting model we envision differs fundamentally from those previously proposed (e.g., Marsh & Carmichael, 1974; Myers *et al.*, 1985; Brophy & Marsh, 1986). By far the greatest contribution from the slab will be in LILE and light REE. The dominant source of Sr, Pb, and Nd enrichments

(relative to Yb) in arc volcanic rocks will commonly be the basalt–gabbro portion of the subducting oceanic crust. Relatively minor contributions of these elements from subducted sediment or by crustal assimilation will, however, produce significant variation in isotopic ratios compared with the dominantly MORB source.

ACKNOWLEDGEMENTS

This study constitutes a portion of Gene Yogodzinski's Ph.D. dissertation at Cornell University. R. W. Kay and S. M. Kay assisted on this project, and reviewed early versions of the manuscript. Discussions with P. B. Kelemen, W. M. White, and T. Plank, and helpful reviews by T. H. Green and R. J. Arculus, are gratefully acknowledged. Support for this research was provided by the National Science Foundation (Grant EAR-9104964). The efforts of the captain and crew of the Russian research vessel *Vulkanolog* are also gratefully acknowledged. Valuable assistance in the field was provided by the US Coast Guard on Attu and Kodiak Islands. Thanks are also due to Michael Cheatham for his efforts in the clean lab–mass spectrometer facilities, and to Howard Aderhold and the crew at the Cornell TRIGA reactor.

REFERENCES

Arculus, R. J. & Powell, R., 1986. Source component mixing in the regions of arc magma generation. *J. Geophys. Res.* **91,** 5913–26.

Arth, J. G., 1976. Behavior of trace elements during magmatic processes—a summary of theoretical models and their applications. *J. Res. U.S. Geol. Surv.* **4,** 41–7.

Baranov, B. C., Seliverstov, N. I., Murav'ev, A. V., & Muzurov, E. L., 1991. The Komandorsky Basin as a product of spreading behind a transform plate boundary. *Tectonophysics* **199,** 237–69.

Bender, J. F., Hodges, F. N., & Bence, A. E., 1978. Petrogenesis of basalts from the project FAMOUS area: experimental study from 0–15 kbars. *Earth Planet. Sci. Lett.* **41,** 277–302.

Borusk, A. M., & Tsvetkov, A. A., 1982. Magmatic associations of the westerm part of the Aleutian Island arc. *Int. Geol. Rev.* **24,** 317–29.

Boyd, T. M., & Creager, K. C., 1991. The geometry of Aleutian subduction: three dimensional seismic imaging. *J. Geophys. Res.* **96,** 2267–91.

Brophy, J. G., & Marsh, B. D., 1986. On the origin of high-alumina arc basalt and the mechanics of melt extraction. *J. Petrology* **27,** 763–89.

Carmichael, I. S. E., 1991. The redox states of basic and silicic magmas: a reflection of their source regions? *Contr. Miner. Petrol.* **106,** 129–41.

Carr, M., Mayfield, D., & Walker, J., 1982. Relation of lava compositions to volcano size and structure in El Salvador. *J. Volcanol. Geotherm. Res.* **10,** 35–48.

Coira, B., & Kay, S. M., 1993. Implications of Quaternary volcanism at Cerro Tuzgle for crustal and mantle evolution of the high Puna Plateau, Central Andes, Argentina. *Contr. Miner. Petrol.* **113,** 40–58.

Conrad, W. K., & Kay, R. W., 1984. Ultramafic and mafic inclusions from Adak Island: crystallization history, and implications for the nature of primary magmas and crustal evolution in the Aleutian arc. *J. Petrology* **25,** 88–125.

Cooper, A. K., Marlow, M. S., Stevenson, A. J., & Scholl, D. W., 1992. Evidence for Cenozoic crustal extension in the Bering Sea region. *Tectonics* **11,** 719–31.

Creager, K. C., & Boyd, T. M., 1991. The geometry of Aleutian subduction: three dimensional kinematic flow model. *J. Geophys. Res.* **96,** 2293–307.

DeBari, S., Kay, S. M., & Kay, R. W., 1987. Ultramafic xenoliths from Adagdak Volcano, Adak, Aleutian Islands, Alaska: deformed igneous cumulates from the MOHO of an island arc. *J. Geol.* **95,** 329–411.

Deer, W. A., Howie, R. A., & Zussman, J., 1966. *An Introduction to Rock-Forming Minerals.* London: Longman, 548 pp.

Defant, M. J., & Drummond, M. S., 1990. Derivation of some modern arc magmas by melting of young subducted lithosphere. *Nature* **347,** 662–5.

DeLong, S. E., & McDowell, F. W., 1975. K–Ar ages from the Near Islands, Western Aleutian Islands, Alaska: indication of a mid-Oligocene thermal event. *Geology* **3,** 691–4.

Dick, H. J. B., & Bullen, T., 1984. Chromian spinel as a petrogenetic indicator in abyssal and alpine-type peridotites and spatially associated lavas. *Contr. Miner. Petrol.* **86,** 54–76.

—— Kelemen, P. B., 1991. Chromian spinel as a petrogenetic indicator of magmagenesis in shallow mantle rocks. (Abstr.) *EOS* **72,** 142.

Eggler, D. H., 1989. Influence of H_2O and CO_2 on melt and fluid chemistry in subduction zones. In: Hart, S. R., & Gulen, L. (eds.) *Crust/Mantle Recycling at Convergence Zones*. Dordrecht: Kluwer Academic, 97–104.

Ellam, R. M., & Hawkesworth, C. J., 1988. Elemental and isotopic variations in subduction related basalts: evidence for a three component model. *Contr. Miner. Petrol.* **98,** 72–80.

Engebretson, D. C., Cox, A., & Gordon, R. G., 1985. Relative motion between oceanic and continental plates in the Pacific Basin. *Geol. Soc. Am. Spec. Paper* **206,** 59 pp.

Falloon, T. J., & Green, D. H., 1987. Anhydrous partial melting of MORB pyrolite and other peridotite compositions at 10 kbar: implications for the origin of primitive MORB glasses. *Miner. Petrol.* **37,** 181–219.

Fisk, M. R., 1986. Basalt magma interaction with harzburgite and the formation of high-magnesium andesites. *J. Geophys, Res.* **13,** 476–70.

Fujimaki, H. M., Tatsumoto, M., & Aoki, K., 1984. Partition coefficients of Hf, Zr, and REE between phenocrysts and groundmasses. *Proc. 14th Lunar Planet. Sci. Conf.*, Part 2. *J. Geophys. Res.* **89** (Suppl.), B662–72.

Geist, E. L., Childs, J. R., & Scholl, D. W., 1988. The origin of summit basins of the Aleutian Ridge: implications for block rotation of an arc massif. *Tectonics* **7,** 327–41.

Gill, J. B., 1987. Early geochemical evolution of an oceanic island arc and backarc: Fiji and the South Fiji Basin. *J. Geol.* **95,** 589–615.

Green, D. H., 1976. Experimental testing of "equilibrium" partial melting of peridotite under water-saturated, high-pressure conditions. *Can. Miner.* **14,** 255–68.

Green, T. H., 1982. Anatexis of mafic crust and high pressure crystallization of andesite. In: Thorpe, R. S. (ed.) *Orogenic Andesites and Related Rocks*. London: John Wiley, 99–114.

—— Pearson, N. J., 1986. Ti-rich accessory phase saturation in hydrous mafic–felsic compositions at high *P*, *T*. *Chem. Geol.* **54,** 185–201.

Gust, D. A., & Perfit, M. R., 1987. Phase relations of a high-Mg basalt from the Aleutian Island arc: implications for primary island arc basalts and high-Al basalts. *Contr. Miner. Petrol.* **97,** 7–18.

Hart, S. R., 1984. A large-scale isotope anomaly in the Southern Hemisphere mantle. *Nature* **309,** 753–7.

—— Reid, M. R., 1991. Rb/Cs fractionation: a link between granulite metamorphism and the S-process. *Geochim. Cosmochim. Acta* **55,** 2379–83.

Hawkins, J. W., Bloomer, S. H., Evans, C., & Melchior, J. T., 1984. Evolution of intra-oceanic arc–trench systems. *Tectonophysics* **102,** 175–205.

Hickey-Vargas, R., 1991. Isotope characteristics of submarine lavas from the Philippine Sea: implications for the origin of arc and basin magmas of the Philippine tectonic plate. *Earth Planet. Sci. Lett.* **107,** 290–304.

Hofmann, A. W., 1988. Chemical differentiation of the earth: the relationship between mantle, continental crust, and oceanic crust. *Ibid.* **90,** 297–313.

—— White, W. M., 1983. Ba, Rb and Cs in the earth's mantle. *Z. Naturforsch.* **38,** 256–66.

Hughes, S. S., 1990. Mafic magmatism and associated tectonism of the Central High Cascade Range, Oregon. *J. Geophys. Res.* **95,** 19 623–38.

—— Taylor, E. M., 1986. Geochemistry, petrogenesis, and tectonic implications of central High Cascade mafic platform lavas. *Geol. Soc. Am. Bull.* **97,** 1024–36.

Jaques, A. L., & Green, D. H., 1980. Anhydrous melting of peridotite at 0–15 Kb pressure and the genesis of tholeiitic basalts. *Contr. Miner. Petrol.* **73,** 287–310.

Kay, R. W., 1978. Aleutian magnesian andesites: melts from subducted Pacific Ocean crust. *J. Volcanol. Geotherm. Res.* **4,** 117–32.

—— 1980. Volcanic arc magma genesis: implications for element recycling in the crust–upper mantle system. *J. Geol.* **88,** 497–522.

—— Kay, S. M., 1988. Crustal recycling and the Aleutian arc. *Geochim. Cosmochim. Acta* **52,** 1351–9.

—— Rubenstone, J. L., & Kay, S. M., 1986. Aleutian terranes from Nd isotopes. *Nature* **322,** 605–9.

Kay, S. M., & Kay, R. W., 1985. Aleutian tholeiitic and calc-alkaline magma series I: the mafic phenocrysts. *Contr. Miner. Petrol.* **90,** 276–90.

—— —— in press. Aleutian magmas in space and time. In: Plafker, G., & Jones, D. L. (eds.) *Geological Society of America Decade of North American Geology, Geology of Alaska, GNA-G1*. Boulder, CO: Geological Society of America.

—— —— Citron, G. P., 1982. Tectonic controls on tholeiitic and calc-alkaline magmatism in the Aleutian arc. *J. Geophys. Res.* **87,** 4051–72.

—— Maksaev, V., Moscoso, R., Mpodozis, C., & Nasi, C., 1987. Probing the evolving Andean lithosphere: mid–late Tertiary magmatism in Chile (29–30°30'S) over the modern zone of subhorizontal subduction. *Ibid.* **92,** 6173–89.

Kelemen, P. B., 1986. Assimilation of ultramafic rock in subduction-related magmatic arcs. *J. Geol.* **94,** 829–43.

—— 1990. Reaction between ultramafic rock and fractionating basaltic magma I. Phase relations, the origin of calc-alkaline magma series, and the formation of discordant dunite. *J. Petrology* **31,** 51–98.

—— Ghiorso, M. S., 1986. Assimilation of peridotite in calc-alkaline plutonic complexes: evidence from the Big Jim Complex, Washington Cascades. *Contr. Miner. Petrol.* **94,** 12–28.

—— Johnson, K. T. M., Kinzler, R. J., & Irving, A. J., 1990. High-field-strength element depletions in arc basalts due to mantle–magma interaction. *Nature* **345,** 521–4.

Klein, E. M., & Langmuir, C. H., 1987. Global correlations of ocean ridge basalt chemistry with axial depth and crustal thickness. *J. Geophys. Res.* **92,** 8089–115.

Lange, R. A., & Carmichael, I. S. E., 1990. Hydrous basaltic andesites associated with minette and related lavas in western Mexico. *J. Petrology* **31,** 1225–59.

Leeman, W. P., 1983. The influence of crustal structure of compositions of subduction-related magmas. *J. Volcanol. Geotherm. Res.* **13,** 561–88.

Lopez, R., & Cameron, K. L., 1992. Miocene high magnesium basaltic andesites from the Gila Bend Mountains, Southwestern Arizona, and their lithospheric source. (Abstr.). *EOS* **73,** 658.

Lugmair, G. W., & Carlson, R. W., 1978. The Sm–Nd history of KREEP. *Proc. 9th Lunar Planet. Sci. Conf. Geochim. Cosmochim. Acta Suppl.* **10,** 689–704.

Luhr, J. F., & Carmichael, I. S. E., 1985. Jorullo Volcano, Michoacan, Mexico (1759–1774): the earliest stages of fractional crystallization in calc-alkaline magmas. *Contr. Miner. Petrol.* **90,** 142–61.

Marsh, B. D., & Carmichael, I. S. E., 1974. Benioff zone magmatism. *J. Geophys. Res.* **79,** 1196–205.

McCulloch, M. T., & Gamble, J. A., 1991. Geochemical and geodynamical constraints on subduction zone magmatism. *Earth Planet. Sci. Lett.* **102,** 358–74.

McDonough, W. F., 1990. Constraints on the composition of the continental lithospheric mantle. *Ibid.* **101,** 1–18.

McKenzie, D., 1984. Generation and compaction of partially molten rock. *J. Petrology* **25,** 713–65.

—— O'Nions, R. K., 1991. Partial melt distributions from inversion of rare earth element concentrations. *Ibid.* **32,** 1021–91.

Michael, P. J., 1988. The concentration, behavior and storage of H_2O in the suboceanic upper mantle: implications for mantle metasomatism. *Geochim. Cosmochim. Acta* **52,** 555–6.

Miller, D. M., Langmuir, C. H., Goldstein, S. L., & Franks, A. L., 1992. The importance of parental magma composition to calc-alkaline and tholeiitic evolution: evidence from Umnak Island in the Aleutians. *J. Geophys. Res.* **97,** 321–43.

Miyashiro, A., 1974. Volcanic rock series in island arcs and active continental margins. *Am. J. Sci.* **274,** 321–55.

Morris, J. D., & Hart, S. R., 1983. Isotopic and incompatible trace element constraints on the genesis of island arc volcanics from Cold Bay and Amak Island, Aleutians, and implications for mantle structure. *Geochim. Cosmochim. Acta* **47,** 2015–30.

—— Leeman, W. P., & Tera, F., 1990. The subducted component in island arc lavas: constraints from Be isotopes and B–Be systematics. *Nature* **344,** 31–5.

Myers, J. D., Marsh, B. D., & Sinha, A. K., 1985. Strontium isotopic and selected trace element variations between two Aleutian volcanic centers (Adak and Atka): implications for the development of arc volcanic plumbing systems. *Contr. Miner. Petrol.* **91,** 221–34.

Nagasawa, H., 1970. Rare earth concentrations in zircons and apatites and their host dacites and granites. *Earth Planet. Sci. Lett.* **9,** 359–64.

—— Schnetzler, C. C., 1971. Partitioning of rare earth, alkali and alkaline earth elements between phenocrysts and acidic igneous rocks. *Geochim. Cosmochim. Acta* **35,** 953–68.

Nakamura, E., Campbell, I. H., & McCulloch, M. T., 1989. Chemical geodynamics in a back arc region around the Sea of Japan: implications for the genesis of alkaline basalts in Japan, Korea, and China. *J. Geophys. Res.* **94,** 4634–54.

Newberry, J. T., Laclair, D. L., & Fujitza, K., 1986. Seismicity and tectonics of the far Western Aleutian Islands. *J. Geodyn.* **6,** 13–32.

Nye, C. J., & Reid, M. R., 1986. Geochemistry of primary and least fractionated lavas from Okmok Volcano, Central Aleutians: implications for arc magmagenesis. *J. Geophys. Res.* **91,** 10 271–87.

Perfit, M. R., & Kay, R. W., 1986. Comment on isotopic and incompatible element constraints on the genesis of island arc volcanics from Cold Bay and Amak Island, Aleutians, and implications for mantle structure. *Geochim. Cosmochim. Acta* **50,** 477–81.

Plank, T., & Langmuir, C. H., 1988. An evaluation of the global variations in the major element chemistry of arc basalts. *Earth Planet. Sci. Lett.* **90,** 349–70.

Poreda, R., & Craig, H., 1989. Helium isotope ratios in circum-Pacific volcanic arcs. *Nature* **338,** 473–8.

Rapp, R. P., Watson, E. B., & Miller, C. F., 1991. Partial melting of amphibolite/eclogite and the origin of Archean trondhjemites and tonalites. *Precambrian Res.* **51,** 1–25.

Reagan, M. K., & Gill, J. B., 1989. Coexisting calcalkaline and high-niobium basalts from Turrialba Volcano, Costa Rica: implications for residual titanates in arc magma sources. *J. Geophys. Res.* **94,** 4619–33.

Ringwood, A. E., 1974. The petrological evolution of island arc systems. *J. Geol. Soc. Lond.* **130,** 183–204.

—— 1990. Slab–mantle interactions 3: Petrogenesis of intraplate magmas and structure of the upper mantle. *Chem. Geol.* **82,** 187–207.

Romick, J. D., Kay, S. M., & Kay, R. W., 1992. The influence of amphibole fractionation on the evolution of calc-alkaline andesite and dacite tephra from the Central Aleutians, Alaska. *Contr. Miner. Petrol.* **112,** 101–18.

—— Tsvetkov, A. A., & Seliverstov, N. I., in press. Silicic volcanism in the Komandorski Basin: evidence for storage of a slab component in the back-arc mantle. *J. Geophys. Res.*

Ryerson, F. J., & Watson, E. B., 1987. Rutile saturation in magmas: implications for Ti–Nb–Ta depletion in island-arc basalts. *Earth Planet. Sci. Lett.* **86,** 225–39.

Salters, V. J. M., & Shimizu, N., 1988. World-wide occurrence of HFSE-depleted mantle. *Geochim. Cosmochim. Acta* **52,** 2177–82.

Saunders, A. D., Rogers, G., Marriner, G. F., Terrell, D. J., & Verma, S. P., 1987. Geochemistry of Cenozoic volcanic rocks, Baja California, Mexico: implications for the petrogenesis of post-subduction magmas. *J. Volcanol. Geotherm. Res.* **32,** 223–45.

Scholl, D. W., Marlow, M. S., MacLeod, N. S., & Buffington, E. C., 1976. Episodic Aleutian Ridge igneous activity: implications of Miocene and younger submarine volcanism west of Buldir Island. *Geol. Soc. Am. Bull.* **87,** 547–54.

—— Vallier, T. L., & Stevenson, A. J., 1987. Geologic evolution and petroleum geology of the Aleutian ridge. In: Scholl, D. W., Grantz, A., & Vedder, J. G. (eds.) *Geology and Resource Potential of the Continental Margin of Western North America and Adjacent Ocean Basins—Beaufort Sea to Baja California.* Houston: Circum-Pacific Council on Energy and Mineral Resources, 103–22.

Seliverstov, N. I., Avdieko, G. P., Ivanenko, A. N., Shkira, V. A., & Khubunaya, S. A., 1990. A new submarine volcano in the west of the Aleutian Island arc. *Volcanol. Seismol.* **8,** 473–95.

Singer, B. F., & Myers, J. D., 1992. Intra-arc extension and magmatic evolution in the central Aleutian arc, Alaska. *Geology* **18,** 1050–3.

Stern, R. J., Morris, J., Bloomer, S. H., & Hawkins, J. W., 1991. The source of the subduction component in convergent margin magmas: trace element and radiogenic evidence from Eocene boninites, Mariana forearc. *Geochim. Cosmochim. Acta* **55,** 1467–81.

Sun, S. S., & McDonough, W. F., 1989. Chemical and isotopic systematics of oceanic basalts: implications for mantle composition and processes. In: Saunders, A. D., & Norry, M. J. (eds.) *Magmatism in the Ocean Basins.* Oxford: Blackwell Scientific, 313–46.

—— Nesbitt, R. W., & Sharaskin, A. Y., 1979. Geochemical characteristics of mid-ocean ridge basalts. *Earth Planet. Sci. Lett.* **44,** 119–38.

Tatsumoto, M., & Nakamura, Y., 1991. DUPAL anomaly in the Sea of Japan: Pb, Nd, and Sr isotopic variations in the eastern Eurasian continental margin. *Geochim. Cosmochim. Acta* **55,** 3697–709.

Tatsumi, Y., 1982. Origin of high-magnesium andesites in the Setouchi volcanic belt, southwest Japan, II: Melting phase relations at high pressure. *Earth Planet. Sci. Lett.* **60,** 305–17.

—— Hamilton, D. L., & Nesbitt, R. W., 1986. Chemical characteristics of fluid phase released from a subducted lithosphere and origin of arc magmas: evidence from high-pressure experiments and natural rocks. *J. Volcanol. Geotherm. Res.* **29,** 293–309.

—— Ishizaka, K., 1982. Origin of high-magnesium andesites in the Setouchi volcanic belt, southwest Japan, I. Petrographical and chemical characteristics. *Earth Planet. Sci. Lett.* **60,** 293–304.

Thompson, G., Bryan, W. B., & Melson, W. G., 1980. Geological and geophysical investigation of the Mid-Cayman Rise Spreading Center: geochemical variation and petrogenesis of basalt glasses. *J. Geol.* **88,** 41–55.

Tsvetkov, A. A., 1991. Magmatism of the westernmost (Komandorsky) segment of the Aleutian Island Arc. *Tectonophysics* **19,** 289–317.

Vallier, T. L., Scholl, D. W., Fisher, M. A., von Huene, R., Bruns, T. R., & Stevenson, A. J., in press. Geologic framework of the Aleutian Arc. In: Plafker, G. & Jones, D. L. (eds.) *Geological Society of America Decade of North American Geology, Geology of Alaska, GNA-G1.* Boulder, CO: Geological Society of America.

Verma, S. P., & Nelson, S. A., 1989. Isotopic and trace element constraints on the origin and evolution of alkaline and calc-alkaline magmas in the northwestern Mexican Volcanic Belt. *J. Geophys. Res.* **94,** 4531–44.

Volynets, O. N., Koloskov, A. V., Yogodzinski, G. M., Seliverstov, N. I., Igorov, V. O., Shkira, V. A., & Matvenkov, V. V., 1992. Boninitic tendencies in lavas of the submarine Piip Volcano and surrounding area (far Western Aleutians): geology, petrochemistry, and mineralogy (in Russian). *Volcanol. Seismol.* No. 1, 3–19.

Walker, R. J., Carlson, R. W., Shirey, S. B., & Boyd, F. R., 1989. Os, Sr, Nd, and Pb isotope systematics of southern African peridotite xenoliths: implications for the chemical evolution of subcontinental mantle. *Geochim. Cosmochim. Acta* **53,** 1583–95.

Wasserburg, G. J., Jacobsen, S. B., DePaolo, D. J., McCulloch, M. T., & Wen, T., 1981. Precise determination of Sm/Nd ratios, Sm and Nd isotopic abundances in standard solutions. *Ibid.* **45,** 2311–23.

Watson, E. B., & Brenan, J. M., 1987. Fluids in the lithosphere, 1. Experimentally-determined wetting characteristics of CO_2–H_2O fluids and their implications for fluid transport, host-rock physical properties, and fluid inclusion formation. *Earth Planet. Sci. Lett.* **85,** 497–515.

White, W. M., Cheatham, M. M., & Duncan, R. A., 1990. Isotope geochemistry of Leg 115 basalts and inferences on the history of the Reunion mantle plume. In: Duncan, R. A., Backman, J., Peterman, L. C., *et al.* (eds.), *Proc. Ocean Drilling Program, Sci. Result.* College Station, TX: Ocean Drilling Program, 53–61.

—— Hofmann, A. W., & Puchelt, H., 1987. Isotope geochemistry of Pacific mid-ocean ridge basalt. *J. Geophys. Res.* **92,** 4881–93.

Yogodzinski, G. M., Kay, R. W., Kay, S. M., Volynets, O. N., & Koloskov, A. V., in prep. Slab melting and magnesian andesites in the Western Aleutian Komandorsky region: implications for modern and Archean subduction systems.

—— Rubenstone, J. L., Kay, S. M., & Kay, R. W., 1993. Magmatic and tectonic development of the Western Aleutians: an oceanic arc in a strike-slip setting. *J. Geophys. Res.* **98,** 11807–34.

APPENDIX: *Dredge locations and descriptions*

Dredge no.	*Location**	*Coordinates*		*Depth interval (m)*	*Mass (kg)*	*Characteristics†*
1. V35-1	Top of north cone of Piip Volcano	55°25·6′N 55°25·2′N	167°16·1′E 167°16·1′E	400–600	>500	Angular blocks of andesite, rare dacite
2. V35-2	North slope of Piip Volcano	55°27·0′N 55°26·4′N	167°16·2′E 167°16·2′E	1200–1620	6	One large angular block of andesite
3. V35-3	West slope of Piip Volcano	55°24·7′N 55°24·6′N	167°11·5′E 167°12·7′E	1460–1840	40–50	Angular blocks and fragments of dacite pumice, misc. stones
4. V35-4	Extrusion at west foot of Piip Volcano	55°26·0′N 55°25·8′N	167°9·8′E 167°10·4′E	1300–1940	150	Angular blocks and fragments of dense dacite lava with andesite xenoliths
5. V35-5	Extrusion at west foot of Piip Volcano	55°27·3′N 55°27·3′N	167°10·0′E 167°10·1′E	2100–2400	20–25	Angular blocks and fragments of dense Mg-andesite, misc. stones
6. V35-6	Western part of Vulkanologist's Massif	55°29·3′N 55°28·7′N	167°6·7′E 167°6·4′E	2140–2300	2	Angular fragments of vesicular andesite with Fe–Mn rinds 1–2 cm thick, misc. stones
7. V35-7	Western part of Vulkanologist's Massif	55°27·9′N 55°28·4′N	167°6·2′E 167°6·8′E	2200–2350	300	Angular blocks and fragments of vesicular andesite and poorly lithified, clay-rich sediments
8. V35-8	Eastern part of Vulkanologist's Massif	55°20·6′N 55°20·6′N	167°27·5′E 167°26·5′E	2100–2400	150	Angular blocks and fragments of vesicular andesite
9. V35-10	Eastern part of Vulkanologist's Massif	55°21·2′N 55°20·6′N	167°25·2′E 167°26·5′E	2100–2500	150	Dense basaltic andesites and andesites, minor Fe–Mn crusts

*See also Fig. 3.

†Blocks are >15 cm in average dimension, fragments <15 cm in average dimension. Miscellaneous stones include rounded and generally weathered volcanic, sedimentary, and metamorphic rocks. These are presumed to be ice rafted.